



**estec**

European Space Research  
and Technology Centre  
Keplerlaan 1  
2201 AZ Noordwijk  
The Netherlands  
T +31 (0)71 565 6565  
F +31 (0)71 565 6040  
[www.esa.int](http://www.esa.int)

# LISA Science Requirements Document

<b>Prepared by</b>	<b>LISA Science Study Team</b>
<b>Reference</b>	<b>ESA-L3-EST-SCI-RS-001</b>
<b>Issue/Revision</b>	<b>1.0</b>
<b>Date of Issue</b>	<b>14th May 2018</b>
<b>Status</b>	<b>Issued (None) ((None)) (None)</b>



# APPROVAL

<b>Title</b> LISA Science Requirements Document	
<b>Issue Number</b> 1	<b>Revision Number</b> 0
<b>Author</b> LISA Science Study Team	<b>Date</b> 14th May 2018
<b>Approved by</b>	<b>Date of Approval</b>

# CHANGE LOG

Reason for change	Issue Nr.	Revision Number	Date
-------------------	-----------	-----------------	------

# CHANGE RECORD

<b>Issue Number</b> 1	<b>Revision Number</b> 0		
Reason for change	Date	Pages	Paragraphs(s)

# DISTRIBUTION

Name/Organisational Unit
--------------------------



**Contents**

**1 EXECUTIVE SUMMARY . . . . . 8**

**2 SCIENCE OBJECTIVES . . . . . 9**

2.1 Introduction . . . . . 9

2.1.1 Notation . . . . . 9

2.1.2 Signals . . . . . 9

2.1.3 Science goals . . . . . 9

2.2 Deriving measurement requirements . . . . . 11

**3 MISSION PERFORMANCE REQUIREMENTS . . . . . 12**

3.1 Sensitivity . . . . . 12

3.2 Strain requirements . . . . . 12

3.3 Observatory response at high frequencies . . . . . 13

3.4 Polarisation . . . . . 13

3.5 Data streams . . . . . 13

3.5.1 Independent sensing channels . . . . . 13

3.5.2 Null stream . . . . . 13

3.6 Mission lifetime . . . . . 14

3.7 Data and data products . . . . . 14

3.7.1 High-priority science data streams . . . . . 14

3.7.2 Auxilliary science data streams . . . . . 14

3.7.3 Science housekeeping data . . . . . 14

3.7.4 Data latency . . . . . 14

3.7.5 Data quality . . . . . 14

3.8 Protected periods . . . . . 16

**APPENDIX A DETAILED RATIONALES . . . . . 17**

SO 1: Study the formation and evolution of compact binary stars in the Milky Way Galaxy. 17

SI 1.1: Elucidate the formation and evolution of Galactic Binaries by measuring their period, spatial and mass distributions. . . . . 18

SI 1.2: Enable joint gravitational and electromagnetic observations of GBs to study the interplay between gravitational radiation and tidal dissipation in interacting stellar systems. . . . . 18

SO 2: Trace the origin, growth and merger history of massive black holes across cosmic ages 20

SI 2.1: Search for seed black holes at cosmic dawn . . . . . 21

SI 2.2: Study the growth mechanism of MBHs before the epoch of reionization . . . 21

SI 2.3: Observation of EM counterparts to unveil the astrophysical environment around merging binaries . . . . . 23

SI 2.4: Test the existence of Intermediate Mass Black Hole Binaries (IMBHBs) . . . 25

SO 3: Probe the dynamics of dense nuclear clusters using EMRIs . . . . . 30

SI 3.1: Study the immediate environment of Milky Way like MBHs at low redshift . 30

SO 4: Understand the astrophysics of stellar origin black holes . . . . . 31

SI 4.1: Study the close environment of SOBHs by enabling multi-band and multi-messenger observations at the time of coalescence . . . . . 31



SI 4.2: Disentangle SOBH binary formation channels . . . . .	31
SO 5: Explore the fundamental nature of gravity and black holes . . . . .	34
SI 5.1: Use ring-down characteristics observed in MBHB coalescences to test whether the post-merger objects are the black holes predicted by GR. . . . .	34
SI 5.2: Use EMRIs to explore the multipolar structure of MBHs . . . . .	36
SI 5.3: Testing for the presence of beyond-GR emission channels . . . . .	36
SI 5.4: Test the propagation properties of GWs . . . . .	36
SI 5.5: Test the presence of massive fields around massive black holes with masses larger than $10^3 M_{\odot}$ . . . . .	36
SO 6: Probe the rate of expansion of the Universe . . . . .	39
SI 6.1: Measure the dimensionless Hubble parameter by means of GW observations only	39
SI 6.2: Constrain cosmological parameters through joint GW and EM observations .	39
SO 7: Understand stochastic GW backgrounds and their implications for the early Universe and TeV-scale particle physics . . . . .	40
SI 7.1: Characterise the astrophysical stochastic GW background . . . . .	40
SI 7.2: Measure, or set upper limits on, the spectral shape of the cosmological stochastic GW background . . . . .	40
SO 8: Search for GW bursts and unforeseen sources . . . . .	42
SI 8.1: Search for cusps and kinks of cosmic strings . . . . .	42
SI 8.2: Search for unmodelled sources . . . . .	42
<b>APPENDIX B SUMMARY . . . . .</b>	<b>43</b>
<b>ACRONYMS . . . . .</b>	<b>44</b>



**List of Figures**

1	Mission constraints on the sky, inclination and polarisation-averaged strain sensitivity	12
2	Massive black hole binary coalescences . . . . .	20
3	Frequency domain waveform of the reference source. . . . .	22
4	A plot of accumulated SNR versus frequency for the reference source. . . . .	22
5	Instantaneous frequency of the reference source as a function of time to merger. The shaded region shows the time in-band. . . . .	22
6	A plot of accumulated SNR versus time to merger for the reference source. . . . .	22
7	Strain sensitivity . . . . .	22
8	Characteristic strain sensitivity . . . . .	22
9	Frequency domain waveform of the reference source. . . . .	24
10	A plot of accumulated SNR versus frequency for the reference source. . . . .	24
11	Instantaneous frequency of the reference source as a function of time to merger. The shaded region shows the time in-band. . . . .	24
12	A plot of accumulated SNR versus time to merger for the reference source. . . . .	24
13	Strain sensitivity . . . . .	24
14	Characteristic strain sensitivity . . . . .	24
15	Frequency domain waveform of the reference source. . . . .	26
16	A plot of accumulated SNR versus frequency for the reference source. . . . .	26
17	Instantaneous frequency of the reference source as a function of time to merger. The shaded region shows the time in-band. . . . .	26
18	A plot of accumulated SNR versus time to merger for the reference source. . . . .	26
19	Strain sensitivity. . . . .	26
20	Characteristic strain sensitivity . . . . .	26
21	Frequency domain waveform of the reference source. . . . .	28
22	A plot of accumulated SNR versus frequency for the reference source. . . . .	28
23	Instantaneous frequency of the reference source as a function of time to merger. The shaded region shows the time in-band. . . . .	28
24	A plot of accumulated SNR versus time to merger for the reference source. . . . .	28
25	Strain sensitivity . . . . .	28
26	Characteristic strain sensitivity . . . . .	28
27	Frequency domain waveform of for the reference source. . . . .	29
28	A plot of accumulated SNR versus frequency for the reference source. . . . .	29
29	Instantaneous frequency of the reference source as a function of time to merger. The shaded region shows the time in-band. . . . .	29
30	A plot of accumulated SNR versus time to merger for the reference source. . . . .	29
31	Strain sensitivity . . . . .	29
32	Characteristic strain sensitivity . . . . .	29
33	Frequency domain waveform of the reference source. . . . .	32
34	A plot of accumulated SNR versus frequency for the reference source. . . . .	32
35	Instantaneous frequency of the reference source as a function of time to merger. The shaded region shows the time in-band. . . . .	32
36	A plot of accumulated SNR versus time to merger for the reference source. . . . .	32
37	Strain sensitivity . . . . .	32
38	Characteristic strain sensitivity . . . . .	32



39	Frequency domain waveform of the reference source. . . . .	35
40	A plot of accumulated SNR versus frequency for the reference source. . . . .	35
41	Instantaneous frequency of the reference source as a function of time to merger. The shaded region shows the time in-band. . . . .	35
42	A plot of accumulated SNR versus time to merger for the reference source. . . . .	35
43	Strain sensitivity . . . . .	35
44	Characteristic strain sensitivity . . . . .	35
45	Frequency domain waveform of the reference source. . . . .	37
46	A plot of accumulated SNR versus frequency for the reference source. . . . .	37
47	Instantaneous frequency of the reference source as a function of time to merger. The shaded region shows the time in-band. . . . .	37
48	A plot of accumulated SNR versus time to merger for the reference source. . . . .	37
49	Strain sensitivity . . . . .	37
50	Characteristic strain sensitivity . . . . .	37



**List of Tables**

1	Overview of science objectives and their respective science investigations . . . . .	10
2	Graphical representation of OR2.1 . . . . .	22
3	Graphical representation of OR2.2 . . . . .	24
4	Graphical representation of OR2.3a . . . . .	26
5	Graphical representation of OR2.4a . . . . .	28
6	Graphical representation of OR2.4b . . . . .	29
7	Graphical representation of OR4.1 . . . . .	32
8	Graphical representation of OR5.1a . . . . .	35
9	Graphical representation of OR5.1b . . . . .	37
10	Spectral indices and gains for the different measurement requirements (MRs) . . . . .	43

## 1 EXECUTIVE SUMMARY

Einstein's theory of spacetime and gravity, General Relativity, predicts that suitably accelerated masses produce propagating vibrations that travel through spacetime at the speed of light. These gravitational waves are produced abundantly in the universe and permeate all of space. Measuring them will add an altogether new way to do astronomy, conveying rich new information about the behaviour, structure, and history of the physical universe, and about physics itself.

LISA is a space mission designed to measure gravitational radiation over a broad band at low frequencies, from about 0.1 mHz to 0.1 Hz, a band where the universe is richly populated by strong sources of gravitational waves (Danzmann and LISA Consortium, 2013). It will measure signals from a wide range of different sources that are of strong interest to the astrophysics of black hole and galaxy formation, to tests of general relativity and to cosmology: massive black holes mergers at all redshifts; extreme mass ratio inspirals; the inspiral of stellar-origin black hole binaries; known binary compact stars and stellar remnants; and probably other sources, possibly including relics of the extremely early Universe, which are as yet unknown.

A major objective of the mission is to determine how and when the massive black holes, present in most galactic nuclei today, have formed and grown over cosmic time. It will explore almost all the mass-redshift parameter space relevant for reconstructing their evolution. The gravitational wave signal from coalescing black holes reveals their spin and redshifted mass, and the distribution of masses and spins will be studied to differentiate between different formation scenarios.

The mission will also study in detail the signals from thousands of stellar-mass close binaries in the Galaxy and give information on the extreme endpoints of stellar evolution. It will provide distances and detailed orbital and mass parameters for hundreds of the most compact binaries, a rich trove of information for detailed mapping and reconstruction of the history of stars in our Galaxy, and a source of information about tidal and non-gravitational influences on orbits associated with the internal physics of the compact remnants themselves.

By observing highly relativistic black hole-black hole coalescences, LISA will provide exceptionally strong tests of the predictions of General Relativity. The signal of merging binary black holes, where maximally warped vacuum spacetimes travel at near the speed of light interacting strongly with each other, allow the study of the full nonlinear dynamics of the theory of gravity. By observing the signal of stellar black holes skimming the horizon of a large massive black hole at the centre of a galaxy, LISA will measure the mass, spin and quadrupole moment of the central object testing its level of Kerrness; thus testing for the first time the black hole hypothesis, and the no-hair conjecture.

Finally, a space-based gravitational wave detector will probe new physics and cosmology, and will search for unforeseen sources of gravitational waves. The LISA frequency band in the relativistic early Universe corresponds to horizon scales where phase transitions of new forces of nature or extra dimensions of space may have caused catastrophic, explosive bubble growth and gravitational wave production.



## 2 SCIENCE OBJECTIVES

### 2.1 Introduction

The science theme of *The Gravitational Universe* is addressed here in terms of science objectives (SOs) that are listed in table 1 and detailed in appendix A. Each SO contains a number of science investigations (SIs) that need to be conducted to fulfill the respective SO.

Each SI comes with operational requirements (ORs) that set the required ability of the observatory, part of which can be expressed in MRs that can be stated in form of strain sensitivities. The stated strain sensitivities always assume *no* further knowledge on the sky position and polarization of the respective source and must therefore be considered as a sky-average and polarization average.

The envelope of the various MRs sets a strain sensitivity requirement for the observatory and is depicted in figure 1 as the dashed line and given quantitatively in equation (3).

The observatory strain sensitivity together with other requirements derived from the ORs are summarised in the mission performance requirements (MPRs).

#### 2.1.1 Notation

The majority of individual LISA sources will be binary systems covering a wide range of masses, mass ratios, and physical states. The GW strain signal  $h(t)$ , also called the waveform, together with its frequency domain representation  $\tilde{h}(f)$ , encodes information about intrinsic parameters of the source in the source frame (*e. g.*, the red-shifted mass  $(1+z)M$  and spin  $\chi$  of the interacting bodies) and extrinsic parameters, such as source inclination  $\iota$ , luminosity distance  $D_L$  and sky location  $(\theta, \phi)$ .

The power spectral density  $S_h(f)$  of the signal  $h(t)$  is estimated by the square of  $\tilde{h}(f)$  scaled with a *measurement bandwidth*,  $f_{\text{MBW}}$ .

$$S_h(f) = \frac{|\tilde{h}(f)|^2}{f_{\text{MBW}}} \quad (1)$$

#### 2.1.2 Signals

Signals are computed according to General Relativity, with redshifts estimated using the cosmological model and parameters inferred from the Planck satellite results (Planck Collaboration et al., 2016). For each class of sources, synthetic models driven by current astrophysical knowledge are used in order to describe their demography. Foregrounds from astrophysical sources as well as backgrounds of cosmological origin are also considered.

#### 2.1.3 Science goals

The performance of the observatory is defined by the MR associated with each OR (see Appendix sA). However, performance *goals* are set which significantly enhance the science return of the mission. These goals shall not drive the mission design, nor are required to be verified during ground testing. Nonetheless, it is required to assess the impact (through analysis) of design and implementation choices as to not knowingly render the observatory incapable of reaching the science goals.

Table 1: Overview of science objectives and their respective science investigations

---

SO 1	<b>Study the formation and evolution of compact binary stars in the Milky Way Galaxy</b>
	<i>SI 1.1 Elucidate the formation and evolution of Galactic Binaries by measuring their period, spatial and mass distributions</i>
	<i>SI 1.2 Enable joint gravitational and electromagnetic observations of galactic binaries (GBs) to study the interplay between gravitational radiation and tidal dissipation in interacting stellar systems</i>
SO 2	<b>Trace the origin, growth and merger history of massive black holes across cosmic ages</b>
	<i>SI 2.1 Search for seed black holes at cosmic dawn</i>
	<i>SI 2.2 Study the growth mechanism of MBHs before the epoch of reionization</i>
	<i>SI 2.3 Observation of EM counterparts to unveil the astrophysical environment around merging binaries</i>
	<i>SI 2.4 Test the existence of intermediate-mass black holes (IMBHs)</i>
SO 3	<b>Probe the dynamics of dense nuclear clusters using extreme mass-ratio inspirals (EMRIs)</b>
	<i>SI 3.1 Study the immediate environment of Milky Way like massive black holes (MBHs) at low redshift</i>
SO 4	<b>Understand the astrophysics of stellar origin black holes</b>
	<i>SI 4.1 Study the close environment of Stellar Origin Black Holes (SOBHs) by enabling multi-band and multi-messenger observations at the time of coalescence</i>
	<i>SI 4.2 Disentangle SOBHs binary formation channels</i>
SO 5	<b>Explore the fundamental nature of gravity and black holes</b>
	<i>SI 5.1 Use ring-down characteristics observed in massive black hole binary (MBHB) coalescences to test whether the post-merger objects are the black holes predicted by General Theory of Relativity (GR)</i>
	<i>SI 5.2 Use EMRIs to explore the multipolar structure of MBHs</i>
	<i>SI 5.3 Testing for the presence of beyond-GR emission channels</i>
	<i>SI 5.4 Test the propagation properties of gravitational waves (GWs)</i>
	<i>SI 5.5 Test the presence of massive fields around massive black holes with masses larger than <math>10^3 M_{\odot}</math></i>
SO 6	<b>Probe the rate of expansion of the Universe</b>
	<i>SI 6.1 Measure the dimensionless Hubble parameter by means of GW observations only</i>
	<i>SI 6.2 Constrain cosmological parameters through joint GW and electro-magnetic (EM) observations</i>
SO 7	<b>Understand stochastic GW backgrounds and their implications for the early Universe and TeV-scale particle physics</b>
	<i>SI 7.1 Characterise the astrophysical stochastic GW background</i>
	<i>SI 7.2 Measure, or set upper limits on, the spectral shape of the cosmological stochastic GW background</i>
SO 8	<b>Search for GW bursts and unforeseen sources</b>
	<i>SI 8.1 Search for cusps and kinks of cosmic strings</i>
	<i>SI 8.2 Search for unmodelled sources</i>

---

## 2.2 Deriving measurement requirements

The assessment of the **operational requirements** requires a calculation of the expected accuracy of the estimation of the parameters of the **GW** and its respective source. Though the Signal-to-Noise Ratio (SNR) is not the only determining factor, it can be used as a good proxy for the expected parameter estimation accuracy. The **SNR** is defined by the frequency integral of the ratio of the signal squared,  $\tilde{h}(f)^2$ , to the strain sensitivity of the observatory, expressed as power spectral density  $S_h(f)$ .

$$\text{SNR}^2 = \int \frac{\tilde{h}(f)^2}{S_h(f)} df \quad (2)$$

The minimum **SNR** above which the required parameter accuracy for a given source can be reached translates into the respective **measurement requirements** for the observatory. Requiring the capability to measure key parameters to some minimum accuracy sets **measurement requirements** that are generally more stringent than those for just detection.

The detailed derivation of the **measurement requirements** from the **operational requirements** is given in Appendix **A**.



$$\begin{aligned}
 S_h(f) &= \frac{1}{2} \frac{20}{3} \left( \frac{S_I(f)}{(2\pi f)^4} + S_{II}(f) \right) \times R(f) \\
 S_I(f) &= 5.76 \times 10^{-48} \frac{1}{\text{s}^4 \text{Hz}} \left( 1 + \left( \frac{f_1}{f} \right)^2 \right) \quad \text{with } f_1 = 0.4 \text{ mHz} \\
 S_{II}(f) &= 3.6 \times 10^{-41} \frac{1}{\text{Hz}} \\
 R(f) &= 1 + \left( \frac{f}{f_2} \right)^2 \quad \text{with } f_2 = 25 \text{ mHz}
 \end{aligned} \tag{3}$$

### 3.3 Observatory response at high frequencies

The requirements above 25 mHz can *only* be exceeded to accommodate the partial cancellation of the effect of the **GW** on the instrument at higher frequencies arising from the length of the interferometer arms, and the subsequent nulls in the observatory response. This also assumes no particular source, in other words, it includes the effects of sky, inclination and polarisation averaging. The envelope of permitted excursions from the required strain sensitivity is expressed as

$$S_h(f) < 2.815 \times 10^{-38} / \text{Hz} \left( 1 + \left( \frac{f}{50 \text{ mHz}} \right)^2 \right) \quad \text{for } f > 25 \text{ mHz.} \tag{4}$$

### 3.4 Polarisation

The observatory shall be able to measure both polarisations of a **GW** simultaneously, i.e., without relying on observatory motion with respect to the source to break the degeneracy.

Observing both polarisations allows some degeneracies in the waveform parameters to be broken leading to significant improvement in parameter estimation and allows an additional degree of freedom of the source to be measured. In particular, extrinsic parameters such as distance and sky position are improved for ‘short’ duration signals ( $\ll$  half a year).

### 3.5 Data streams

#### 3.5.1 Independent sensing channels

The observatory shall provide at least two quasi-independent data streams containing the science observables. (Here, ‘quasi-independent’ refers to the noise properties of the two channels, which may be correlated at some level.) This allows instrumental effects (such as force glitches on a single test mass) to be distinguished from unmodelled astrophysical sources.

#### 3.5.2 Null stream

The mission shall provide a *null stream* to aid in assessing instrumental noise and artefacts. The null stream should be ‘perfect’ for a given source location, but may be frequency dependent for the general case.

### **3.6 Mission lifetime**

The mission lifetime shall accommodate a 4 year science measurement phase. The goal is to make an extension to 10 years possible. Out of the 4 years of science measurement, the duty cycle of usable science data at full (nominal) performance shall be greater than 75%.

### **3.7 Data and data products**

All science data streams discussed below shall be properly acquired employing suitable anti-alias filtering and appropriate resolution of acquisition to ensure the measurements are not limited by (TBD) quantisation noise or aliasing effects in the measurement band.

#### ***3.7.1 High-priority science data streams***

The data streams needed to produce the science observables at the required sensitivity shall be made available for all times when in science observing mode, with the required data rate and at the required resolution. The data rate shall be sufficient to allow for the sensitivity to be achieved over the measurement band-width of 100 mHz with a goal of 1 Hz. implying data at a rate greater than 2 Hz.<sup>1</sup> We refer to such data streams as high-priority science data streams.

#### ***3.7.2 Auxilliary science data streams***

An additional set of data streams needed to monitor physical environment of the observatory to allow for characterisation of the science observables shall be made available at the appropriate (TBD) data rates and resolutions. We refer to such data streams as 'auxilliary science data streams'.

#### ***3.7.3 Science housekeeping data***

Monitoring of critical instrument parameters shall be done via the appropriate set of housekeeping data streams.

#### ***3.7.4 Data latency***

Science data shall be telemetered to ground daily to allow for prompt analysis and monitoring of the observatory performance. Data shall be available from the ESA LISA data archive within TBD hours of reception on ground.

#### ***3.7.5 Data quality***

The quality of the data may be reduced due to the various reasons detailed below. This will impact the detectability of sources as well as the parameter estimation.

---

<sup>1</sup> Preliminary analysis shows that a data telemetered at a rate of 4 Hz is required to allow a useful measurement bandwidth up to 1 Hz. This assumes an initial laser frequency noise of  $30\text{Hz}/\sqrt{\text{Hz}}$ , armlength knowledge of 1 m, phasemeter sampling at 20 Hz, and 200 dB attenuation from anti-aliasing filtering.

### ***Data gaps***

Gaps in the data will affect the science performance in two ways:

- through the duty cycle, which reduces the SNR;
- and through the reduction in the accuracy of parameter estimation (**TBC**) and by introducing biases (**TBC**).

The data still can be analyzed in a fully coherent way, but since matched filtering is usually done in the frequency domain, it requires windowing of the data on both sides of every gap. The windowing should be taken into account when computing the duty cycle. The length of the windows is of order 1 day (**TBD**), independent of the gap length.

The long duration signals are mainly affected through the reduction of SNR (duty cycle), while short signals (< half a year), e.g., Massive Black Hole Binaries (**MBHBs**), are very sensitive to when gaps happen with respect to the merger. The short duration signal will be affected not only due to reduction of SNR but also in degradation of the parameter estimation. The biggest effect of the gaps is on the early warnings for the coalescing **MBHBs**. Long gaps (duration of order a week) will significantly affect the parameter estimation within the last month before the merger of **MBHBs** (**TBC**). Short gaps (of order a few hours) will affect parameter estimation if their frequency is  $> N$  (**TBD**) per month.

Data gaps are anticipated either due to planned interruptions or anomalies. The requirements on any planned gaps are:

- Any periodicity of the interruptions shall not be in band;
- Any planned gaps shall be avoided during any protected periods;
- No data gaps due to planned interruptions of science data taking shall be longer than a few hours (**TBD**) and not more frequent than **TBD**.

Unplanned gaps obviously depend upon probability, reliability of subsystems, etc, but the effect of gaps has a significant impact on science output, and therefore such gaps should be minimised through system reliability, and also by optimising anomaly recovery time.

### ***Non-stationarity***

Two types of non-stationarity of the overall observatory performance needs to be considered: fluctuations in the PSD of observatory sensitivity arising from, e.g., orbital dynamics, temperature variations, and fluctuating magnetic fields; and periods of excess noise due to maintenance or calibration activities.

For fluctuations in the PSD, the system shall be designed to avoid any deliberate sources of disturbance that can lead to non-stationarity in the observatory performance at a level of 10% in power (**TBD**) of the averaged PSD estimated over month time-scales.

The system shall be designed to minimise periods of excess noise arising from deliberate activities, for example, antenna repointing.

### ***Non-Gaussian events (glitches)***

Glitches refer to transient, sporadic events in the system which can lead to transient signals in the science observables. In certain circumstances (**TBD**) it may be impossible to distinguish the source



of such glitches as coming from the instrument (for which the instrument shall have the diagnostic possibilities discussed above in Section 3.5) or an unmodelled astrophysical system. Therefore, the observatory shall be designed to minimise the possibility of such transients.

### ***Spectral lines and coherent noise***

Instrumental sources of quasi-monochromatic signals in the measurement band should be avoided as these are potentially indistinguishable from sources of monochromatic gravitational waves, especially if they have any measurable frequency derivative.

### ***Missing samples***

Constellation science data shall be properly and consistently recorded and telemetered to ground to ensure that science analysis is not affected by missing samples. In addition, proper time-stamping of all science data shall be made at the level of 10 ns (TBD) to allow for accurate, coherent combining of data streams on ground. This implies, for example, that a single clock should be used on each satellite to ensure uniform sampling across different units, and that a system is in place to allow for comparison of clocks on each satellite at the required level.

## **3.8 Protected periods**

It shall be possible to reschedule any planned interruptions of science data taking to allow for a specified *protected period* of up to 14 days starting no sooner than 2 days following the request.<sup>2</sup> This is to ensure that foreseen short-term astrophysical phenomena will not be missed.

For such protected periods, all science data shall be available for analysis at the DPC not later than 24 hours after the measurement occurred.

---

<sup>2</sup>This could be either achieved by advancing or by delaying planned interruptions, depending on the exact scenario, available groundstations etc.



## A DETAILED RATIONALES

The science case of LISA is addressed here in terms of Science Objectives (SOs) and Science Investigations (SIs), and the Observational Requirements (ORs) necessary to reach those objectives. The ORs are in turn related to Mission Requirements (MRs) for the noise performance, mission duration, etc. The assessment of ORs requires a calculation of the Signal-to-Noise-Ratio (SNR) and the parameter measurement accuracy. Requirements for a minimum SNR level, above which a source is detectable, translate into specific MRs for the observatory. The MR requirement has been translated into a gain,  $\alpha$ , and spectral index,  $\beta$  as defined in Section B.

### Definitions

The science objectives listed in this appendix, use the following definitions:

- $\mathbf{M}_{\text{tot}}$ : Total mass of the binary system ( $m_1 + m_2$ ), where  $m_{1/2}$  are the individual masses of the source objects.
- $\mathcal{M}$  - Chirp mass: The chirp mass is used to define the leading order term of the evolution of the amplitude and frequency of the gravitational wave from an inspiralling binary system. The chirp mass is defined as:

$$\mathcal{M} = \frac{(m_1 m_2)^{\frac{3}{5}}}{(m_1 + m_2)^{\frac{1}{5}}}$$

- $\chi$ : Dimensionless spin parameter, defined as:

$$\chi = \frac{c}{G} \frac{S}{m}$$

where  $m$  is the mass and  $S$  is the spin angular momentum of the object.

- $q$ : The mass ratio between the two bodies of the binary system,  $q = m_1/m_2$
- **Characteristic strain**: The characteristic strain is essentially the rms signal in a frequency interval of width  $\Delta f = f$ , centered at frequency  $f$ . It is commonly used when plotting sensitivity curves, as the area between the characteristic strain of the source, and the instrument sensitivity gives a measure of the signal to noise ratio of that particular source.

### SO 1: Study the formation and evolution of compact binary stars in the Milky Way Galaxy.

Numerous compact binaries in the Milky Way galaxy emit continuous and nearly monochromatic GW signals in the source frame (Nelemans et al., 2001). These GBs comprise primarily white dwarfs but also neutron stars and stellar-origin black holes in various combinations. For those systems that can be detected, the orbital periods  $P = 2/f$  can often be measured to high accuracy. The orbital motion of the detector imparts a characteristic frequency and amplitude modulation that allows us to constrain the extrinsic properties of some of the systems. Higher frequency systems are typically louder and better characterized than low frequency systems. At low frequencies, GBs are thought to be so numerous that individual detections are limited by confusion with other binaries yielding a stochastic foreground or confusion signal. Several *verification* binaries are currently known for which joint gravitational and EM observations can be done and many more will be discovered in the coming years, e.g. by Gaia and the Large Synoptic Survey Telescope (LSST). Using the current best estimate for the population

(Toonen et al., 2012), and assuming the reference sensitivity, it should be possible to detect and resolve about 25 000 individual GBs.

***SI 1.1: Elucidate the formation and evolution of Galactic Binaries by measuring their period, spatial and mass distributions.***

***OR 1.1.a:***

To survey the period distribution of GBs, and have the capability to distinguish between about 5000 systems with an inferred period precision of  $\delta P/P < 10^{-6}$ .

***OR 1.1.b:***

To measure the mass, distance and sky location for a significant fraction of these GBs with frequency  $f > 3$  mHz, chirp mass  $\mathcal{M} > 0.2 M_{\odot}$  and distance  $d < 15$  kpc.

***OR 1.1.c:***

To detect the low frequency galactic confusion noise in the frequency band from 0.5 mHz to 3 mHz. In Figure 1, the galactic confusion signal for a fiducial population is shown assuming the nominal mission duration, and after subtraction of individual sources.

**MRI.1:**

The ORs pose requirements in the band from about 0.5 mHz to 30 mHz. OR 1.1b demands that the sensitivity complies to

$$\begin{aligned} \sqrt{S_h(f)} &< 1.7 \times 10^{-20} \text{ Hz}^{-1/2} & \text{at } f = 3 \text{ mHz} \\ \sqrt{S_h(f)} &< 8.1 \times 10^{-20} \text{ Hz}^{-1/2} & \text{at } f = 30 \text{ mHz} \\ \alpha &= 8.37 \times 10^{-21} & \beta = 0.667 \end{aligned} \quad (\text{MR 1.1b})$$

The identification of the low frequency galactic confusion signal requires the ability to subtract all the identified, known sources with a certain precision that is limited by the other unknown sources as well as the detector sensitivity. In order for the detector sensitivity not to limit this significantly, we require the detector noise level below 2 mHz to be at, or below, the combined signal from galactic binaries. Using a conservative estimate for the galactic population sets a limit on the sensitivity to

$$\begin{aligned} \sqrt{S_h(f)} &< 6.2 \times 10^{-19} \text{ Hz}^{-1/2} & \text{at } f = 0.5 \text{ mHz} \\ \sqrt{S_h(f)} &< 2.3 \times 10^{-20} \text{ Hz}^{-1/2} & \text{at } f = 3 \text{ mHz} \\ \alpha &= 1.73 \times 10^{-19} & \beta = -1.83 \end{aligned} \quad (\text{MR 1.1c})$$

***SI 1.2: Enable joint gravitational and electromagnetic observations of GBs to study the interplay between gravitational radiation and tidal dissipation in interacting stellar systems.***

***OR 1.2.a:***

To detect about 10 of the currently known verification binaries, inferring periods with accuracy  $\delta P/P < 1 \times 10^{-6}$ .

***OR 1.2.b:***

To enable identification of possible electromagnetic counterparts, determine the sky location of about 5000 systems within one square degree.

***OR 1.2.c:***

To study the interplay between gravitational damping, tidal heating, and to perform tests of **GR**, localise about 100 systems within one square degree and determine their first period derivative to a fractional accuracy of 10 % or better.

**MR 1.2:**

**ORs 1.1.a, 1.1.b, and 1.2.b and 1.2.c** set requirements on the science observation time in order to achieve the desired measurement precision. These requirements may not be fully met for a science observation time less than four years.

## SO 2: Trace the origin, growth and merger history of massive black holes across cosmic ages

The origin of **MBHs** powering active galactic nuclei (AGN) and lurking at the centres of today's galaxies is unknown. Current studies predict masses for their *seeds* in the interval between about  $10^3 M_{\odot}$ , and a few  $10^5 M_{\odot}$  and formation redshifts  $10 \lesssim z \lesssim 15$  (Volonteri, 2010). They then grow up to  $10^8 M_{\odot}$  and more by accretion episodes, and by repeated merging, thus participating in the clustering of cosmic structures (Sesana et al., 2004), inevitably crossing the entire LISA frequency spectrum, from a few  $10^{-5}$  Hz to  $10^{-1}$  Hz, since their formation redshift.

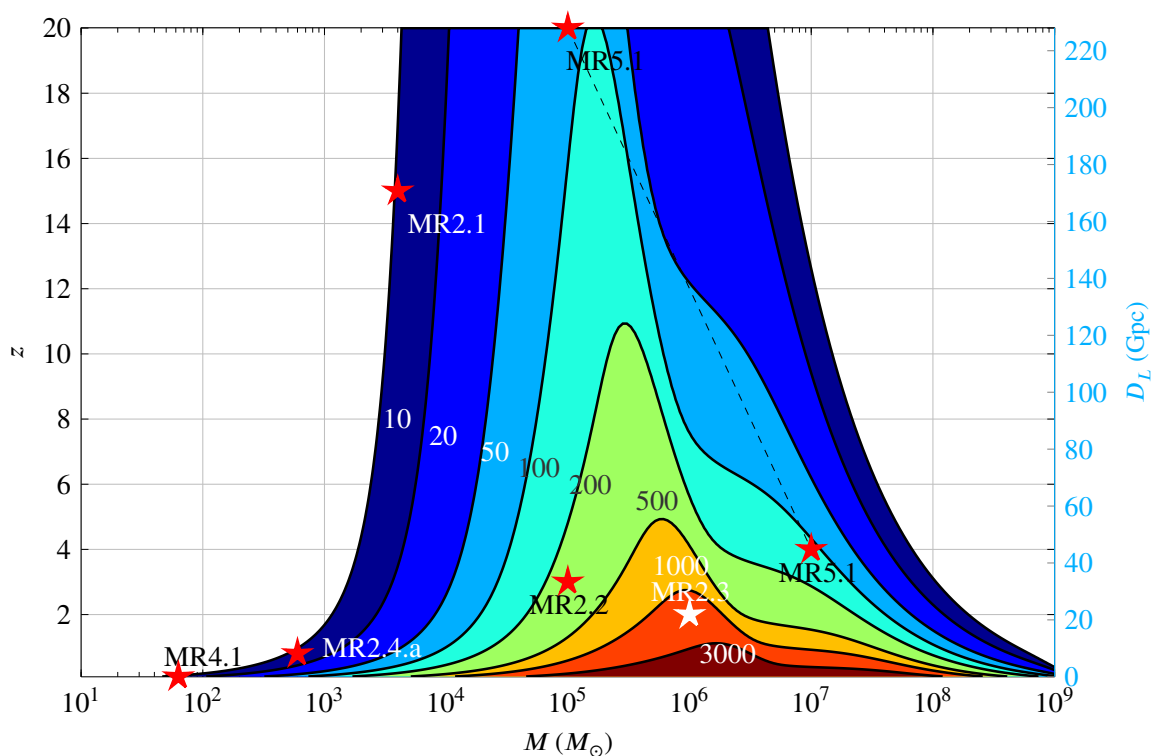


Figure 2: Massive black hole binary coalescences: contours of constant **SNR** for the baseline observatory in the plane of total source-frame mass,  $M$ , and redshift,  $z$  (left margin—assuming Planck cosmology), and luminosity distance,  $D_L$  (right margin), for binaries with constant mass ratio of  $q = 0.2$ . Overlaid are the positions of the threshold binaries used to define the mission requirements.

Mergers and accretion influence their spins in different ways thus informing us about their way of growing. The **GW** signal is transient, lasting from months to days down to hours. The signal encodes information on the inspiral and merger of the two spinning **MBHs** and the ring-down of the new **MBH** that formed. Being sources at cosmological redshifts, masses in the observer frame are  $(1 + z)$  heavier than in the source frame, and source redshifts are inferred from the luminosity distance  $D_L$ , extracted from the signal (with the exception of those sources for which we have an independent measure of  $z$  from an identified electromagnetic counterpart). Consistent with current, conservative population models (Klein et al., 2016), the expected minimum observation rate of a few **MBHB** per year will fulfill the requirements of SO 2.

Figure 2 presents the multitude of sources that should be visible to LISA, showing a wide range of

masses observable with high **SNR** out to high redshift. The definition of the threshold systems (which are shown as red stars in figure 2) for each **OR** leads to one or more **MR**, shown in figure 1.

## ***SI 2.1: Search for seed black holes at cosmic dawn***

### ***OR 2.1***

Have the capability to detect the inspiral of **MBHBs** in the interval between a few  $10^3 M_{\odot}$  and a few  $10^5 M_{\odot}$  in the source frame, and formation redshifts between  $z = 10$  and  $z = 15$ . Enable the measurement of the source frame masses and the luminosity distance with a fractional error of 20 % to distinguish formation models.

### **MR 2.1:**

Ensure the strain sensitivity complies with

$$\begin{aligned}
 \sqrt{S_h(f)} &< 1.6 \times 10^{-20} \text{ Hz}^{-1/2} & \text{at } f = 3 \text{ mHz} \\
 \sqrt{S_h(f)} &< 1.2 \times 10^{-20} \text{ Hz}^{-1/2} & \text{at } f = 10 \text{ mHz} \\
 \alpha &= 2.19 \times 10^{-20} & \beta = -0.261
 \end{aligned}
 \tag{MR 2.1}$$

to enable the observation of binaries at the low end of this parameter space with a **SNR**  $\geq 10$ . Such a “threshold” system would have a mass of  $4000 M_{\odot}$ , mass ratio  $q = 0.2$ , and be located at a redshift of  $z = 15$ . All other **MBHBs** in **OR 2.1** with masses in the quoted range and mass ratios higher than this and/or at lower redshift, will then be detected with higher **SNR** yielding better parameter estimation.

### **Rationale**

The **OR** calls for a range of masses and redshifts. In selecting a threshold binary here, the worst case is the lowest mass, highest redshift, spin of  $\chi = 0$ , and a mass ratio at the limit of what can be easily modeled ( $q = 0.2$ ). The waveform for this “threshold” system is shown in figure 3.

This system enters the band of the observatory (i.e. starts accumulating significant **SNR**) at around 2 mHz and leaves the band (stops accumulating significant amount of **SNR**) around 50 mHz. The accumulated **SNR** as a function of frequency for this system is shown in figure 4. Under the assumed characteristic strain, most of the **SNR** is accumulated from about 2 mHz up to 10 mHz; as the total **SNR** is relatively low, accumulation starts as soon as the signal enters the band. The requirement on the **PSD** of the observatory strain sensitivity is set in a band from 3 mHz to 10 mHz. The resulting **MR** is shown in Figures 7 and 8 expressed in strain sensitivity and characteristic strain, respectively.

## ***SI 2.2: Study the growth mechanism of MBHs before the epoch of reionization***

### ***OR 2.2.a***

Have the capability to detect the signal for coalescing **MBHBs** with mass  $10^4 M_{\odot} < M < 10^6 M_{\odot}$  in the source frame at  $z \lesssim 9$ . Enable the measurement of the source frame masses at the level limited by weak lensing (5 %).

Table 2: Graphical representation of OR2.1. Parameters of the reference source are  $z = 15$ ,  $M_{\text{tot}} = 4 \times 10^3 M_{\odot}$ ,  $q = 0.2$ ,  $\chi = 0$ ; its maximum accumulated SNR is 10.2.

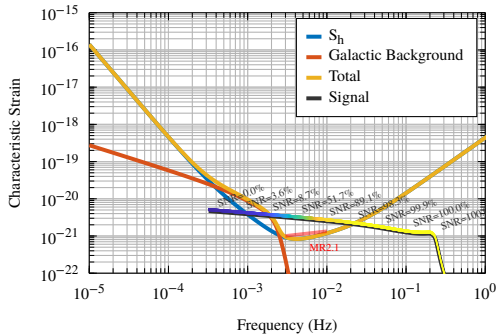


Figure 3: Frequency domain waveform of the reference source.

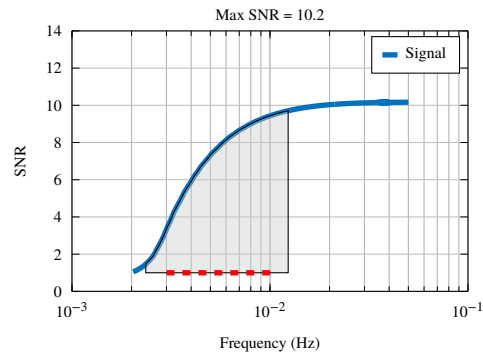


Figure 4: A plot of accumulated SNR versus frequency for the reference source.

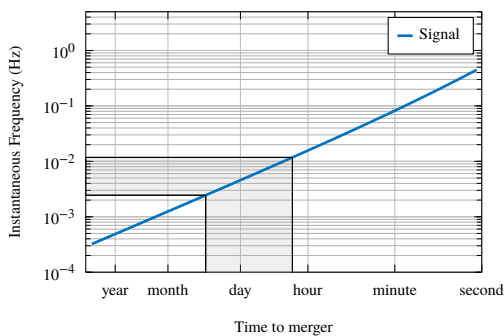


Figure 5: Instantaneous frequency of the reference source as a function of time to merger. The shaded region shows the time in-band.

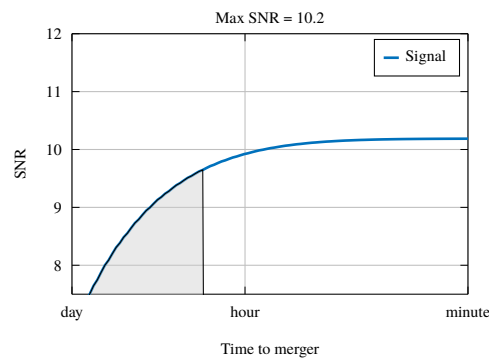


Figure 6: A plot of accumulated SNR versus time to merger for the reference source.

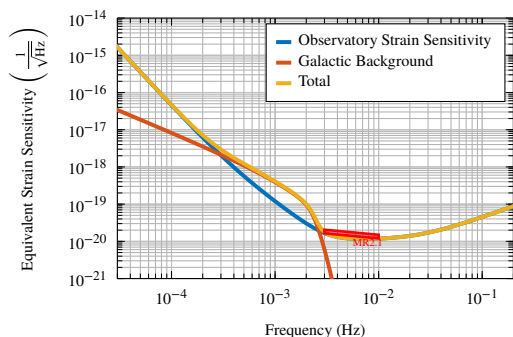


Figure 7: Strain sensitivity

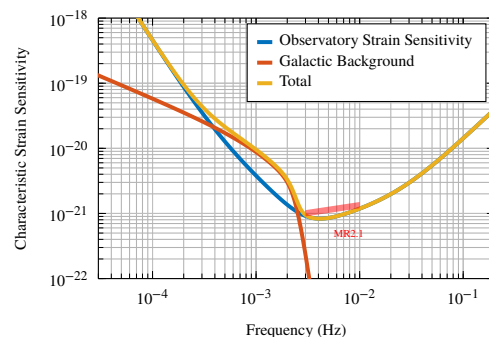


Figure 8: Characteristic strain sensitivity

### **OR 2.2.b**

For sources at  $z < 3$  and  $10^5 M_{\odot} < M < 10^6 M_{\odot}$ , enable the measurement of the dimensionless spin of the largest **MBH** with an absolute error better than 0.1 and the detection of the misalignment of spins with the orbital angular momentum better than 10%. This parameter accuracy corresponds to an accumulated **SNR** (up to the merger) of at least 200.

#### **MR2.2:**

The most stringent requirement is set by being able to measure the spin of a threshold system with total intrinsic mass of  $10^5 M_{\odot}$ , mass ratio of  $q = 0.2$ , located at  $z = 3$ . This will satisfy both **OR 2.2.a** and **2.2.b**.

$$\begin{aligned}
 \sqrt{S_h(f)} &< 1.2 \times 10^{-19} \text{ Hz}^{-1/2} & \text{at } f &= 1 \text{ mHz} \\
 \sqrt{S_h(f)} &< 1.6 \times 10^{-20} \text{ Hz}^{-1/2} & \text{at } f &= 8 \text{ mHz} \\
 \alpha &= 1.23 \times 10^{-19} & \beta &= -0.993
 \end{aligned}
 \tag{MR 2.2}$$

All systems in **OR 2.2.a** and **2.2.b** with higher mass, mass ratios, spins, or lower redshift will result in higher **SNR**, and better spin estimation.

### **Rationale**

The **OR** calls for a range of masses and redshifts. In selecting a threshold binary here, the worst case is again the lowest mass, highest redshift, spin of  $\chi = 0$ , and a mass ratio at the limit of what can be easily modeled ( $q = 0.2$ ). The waveform for the threshold system is shown in figure 9.

This system enters the band of the detector at around 0.2 mHz and leaves the band around 50 mHz. The accumulated **SNR** as a function of frequency for this system is shown in figure 10. From that we see that most of the **SNR** is accumulated between 0.6 mHz and 9 mHz, so we set a requirement on the power spectral density (PSD) of the observatory strain sensitivity from 1 mHz to 8 mHz. The resulting **MR** is shown in Figures 13 and 14 expressed in strain sensitivity and characteristic strain, respectively.

## ***SI 2.3: Observation of EM counterparts to unveil the astrophysical environment around merging binaries***

### **OR 2.3.a**

Observe the mergers **MBHBs** with total masses between  $10^5 M_{\odot}$  and  $10^7 M_{\odot}$  around the peak of star formation ( $z \sim 2$ ), with sufficient **SNR** to allow the issuing of alerts to **EM** observatories with a sky-localisation of  $100 \text{ deg}^2$  at least one day prior to merger. This would yield coincident **EM/GW** observations of the systems involved.

### **OR 2.3.b**

After gravitationally observing the merger of systems discussed in **OR 2.3.a**, the sky localisation will be significantly improved, allowing follow-up EM observations to take place. This has the potential to enable the observation of the formation of a quasar following a **MBHB** merger. This needs excellent sky localisation (about  $1 \text{ deg}^2$ ) to distinguish from other variable EM sources in the field months to years after the merger.



Table 3: Graphical representation of OR2.2. Parameters of the reference source are  $z = 3$ ,  $M_{\text{tot}} = 10^5 M_{\odot}$ ,  $q = 0.2$ ,  $\chi = 0$ ; its maximum accumulated SNR is 262.8.

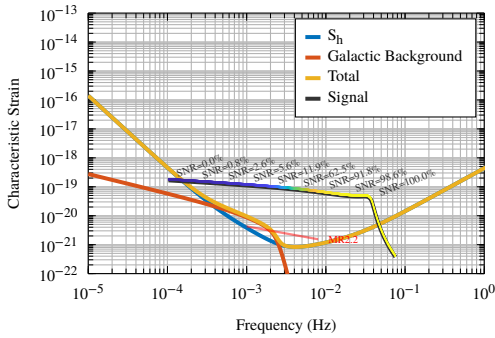


Figure 9: Frequency domain waveform of the reference source.

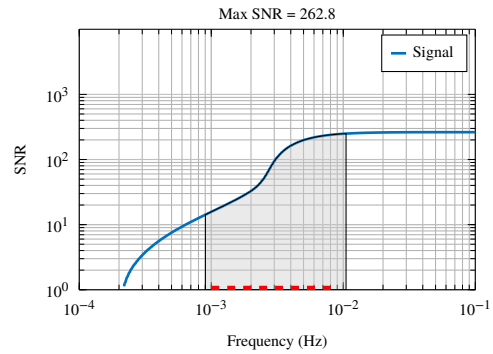


Figure 10: A plot of accumulated SNR versus frequency for the reference source.

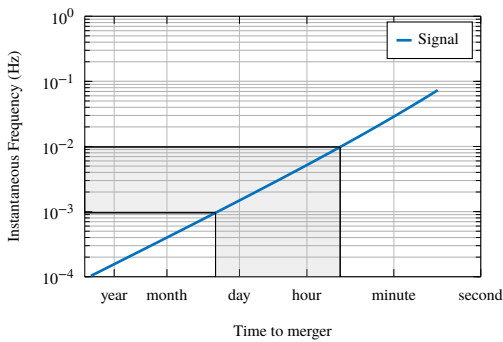


Figure 11: Instantaneous frequency of the reference source as a function of time to merger. The shaded region shows the time in-band.

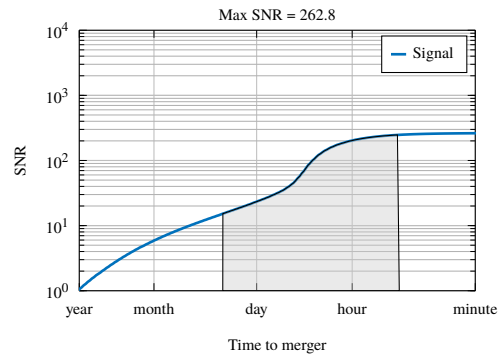


Figure 12: A plot of accumulated SNR versus time to merger for the reference source.

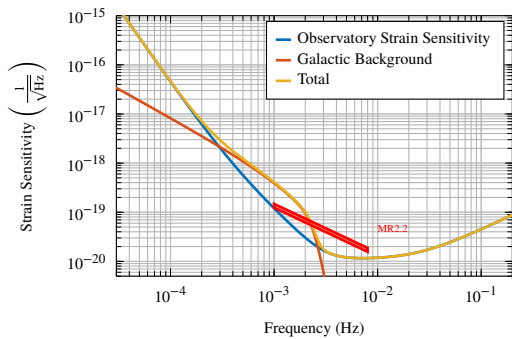


Figure 13: Strain sensitivity

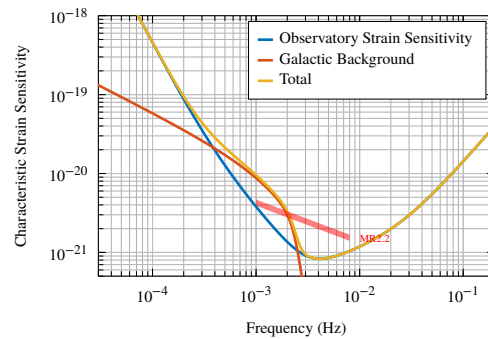


Figure 14: Characteristic strain sensitivity



**MR 2.3:**

For the lowest **SNR** system in OR 2.3.a, which corresponds to a mass of  $10^6 M_{\odot}$  at  $z = 2$ , we will detect the inspiral signal (with an **SNR** of 10) about 13.1 days prior to merger. Localising this source to  $100 \text{ deg}^2$  requires an accumulated **SNR** of about 50, which will be known about 28 hours prior to merger if the strain sensitivity of the observatory follows

$$\begin{aligned}
 \sqrt{S_h(f)} &< 4.5 \times 10^{-17} \text{ Hz}^{-1/2} & \text{at } f &= 0.1 \text{ mHz} \\
 \sqrt{S_h(f)} &< 1.2 \times 10^{-18} \text{ Hz}^{-1/2} & \text{at } f &= 0.37 \text{ mHz} \\
 \alpha &= 7.86 \times 10^{-20} & \beta &= -2.76
 \end{aligned}
 \tag{MR 2.3a}$$

To achieve this operationally, data from the observatory needs to be made available for analysis, around one day after measurement on-board. Additionally, in order to ensure coincident observations of **GW** and **EM**, we need to trigger a “protected period” on-board during which no commissioning activities should take place. Hence there are three **MRs** here: a constraint on the strain sensitivity; a constraint on the cadence with which data are downloaded from the satellites; and the ability to trigger “protected periods” where the instrument configuration is maintained. For all other systems in OR 2.3.a with lower redshift, the **SNR** will be higher, and the sky-localisation correspondingly better.

**Rationale**

The **OR** calls for a range of masses and redshifts. In selecting a threshold binary here, we need to consider the time at which we will detect the signal, and if that is enough time to trigger an alert for prompt **EM** observations.

For the lowest **SNR** system in OR2.3.a, which corresponds to a mass of  $10^6 M_{\odot}$  at  $z = 2$ , we will detect the inspiral signal (with **SNR** = 10) about 11.5 days prior to merger (see figure 18). Localising this source to  $100 \text{ deg}^2$  requires an accumulated **SNR** on average of about 50, which will be collected approximately 32 hours prior to merger for the threshold source. This is compatible with the data download cadence being considered, and a little margin for processing time given the chosen observatory strain requirement.

The threshold system enters the band of the detector at around  $80 \mu\text{Hz}$  and merges in the band. The accumulated **SNR** as a function of frequency for this system is shown in figure 16. The **SNR** is accumulated over the whole band, so the frequency band for the requirement is chosen from the lower end of the band to approximately the onset of the galactic foreground signal. The resulting **MR** is shown in figure 19 and figure 20, expressed in strain sensitivity and characteristic strain, respectively.

***SI 2.4: Test the existence of Intermediate Mass Black Hole Binaries (IMBHBs)******OR 2.4.a:***

Have the ability to detect the inspiral from nearly equal mass Intermediate Mass Black Hole Binaries of total intrinsic mass between  $1000 M_{\odot}$  and  $10^4 M_{\odot}$  at  $z < 1$ , measuring the component masses to a precision of 30 %, which requires a total accumulated **SNR** of at least 20.



Table 4: Graphical representation of OR2.3a. Parameters of the reference source are  $z = 2$ ,  $M_{\text{tot}} = 10^6 M_{\odot}$ ,  $q = 0.2$ ,  $\chi = 0$ ; its maximum accumulated SNR is 1376.6.

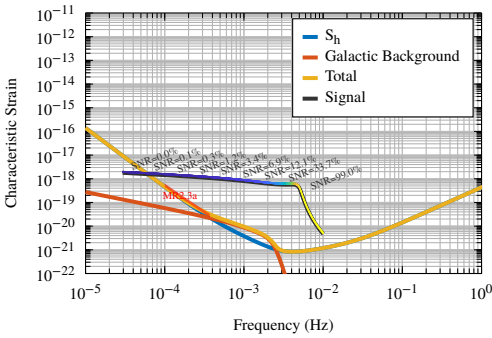


Figure 15: Frequency domain waveform of the reference source.

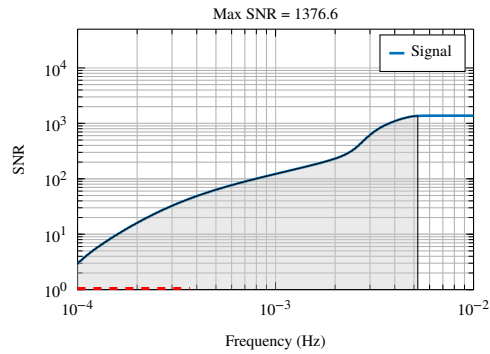


Figure 16: A plot of accumulated SNR versus frequency for the reference source.

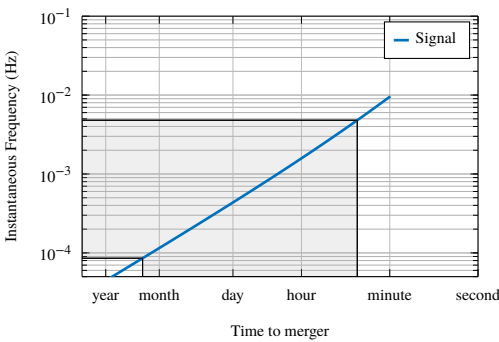


Figure 17: Instantaneous frequency of the reference source as a function of time to merger. The shaded region shows the time in-band.

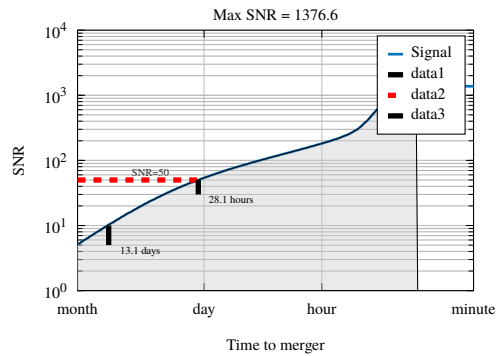


Figure 18: A plot of accumulated SNR versus time to merger for the reference source.

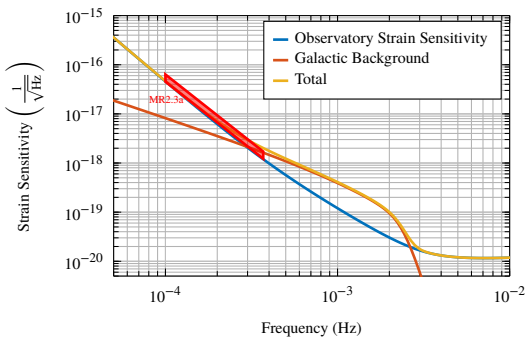


Figure 19: Strain sensitivity.

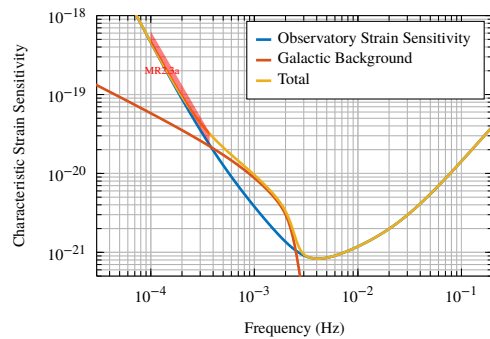


Figure 20: Characteristic strain sensitivity

**MR 2.4.a:**

Achieving a total **SNR** of about 20 for the systems described in OR 2.4.a requires the strain sensitivity of the observatory to comply with

$$\begin{aligned}
 \sqrt{S_h(f)} &< 1.9 \times 10^{-20} \text{ Hz}^{-1/2} & \text{at } f = 3 \text{ mHz} \\
 \sqrt{S_h(f)} &< 1.2 \times 10^{-20} \text{ Hz}^{-1/2} & \text{at } f = 8 \text{ mHz} \\
 \alpha &= 3.32 \times 10^{-20} & \beta = -0.500
 \end{aligned}
 \tag{MR 2.4a}$$

for the threshold system of  $1000 M_\odot$  with a mass ratio of  $q = 1$ , located at  $z = 1$ .

**Rationale**

The threshold system for this **OR** is a  $1000 M_\odot$  symmetric mass binary ( $q = 1$ ) at  $z = 0.8$  that has an **SNR** of 22 under the strain requirements (equation (3)). It enters the detection band around 2 mHz and leaves the band long before merger at around 40 mHz. Figure 21 shows the waveform for this system and figure 22 shows the accumulation of **SNR** as a function of frequency, showing that most of the **SNR** is accumulated in a band from 2 mHz to 8 mHz, which has been set as the relevant band for the requirement.

**OR 2.4.b:**

Have the ability to detect unequal mass **MBHBs** of total intrinsic mass  $10^4 M_\odot$  to  $10^6 M_\odot$  at  $z < 3$  with the lightest black hole (the intermediate-mass black hole (IMBH)) in the intermediate mass range between  $10^2 M_\odot$  and  $10^4 M_\odot$  (Portegies Zwart and McMillan, 2002), measuring the component masses to a precision of 10 %, which requires a total accumulated **SNR** of at least 20.

**MR 2.4.b:**

Systems of OR 2.4.b set constraints on the strain sensitivity of the observatory along the descending branch of the U-shaped curve where the galactic confusion noise-like signal dominates. Achieving a total **SNR** of 20 across that band for the systems described in OR 2.4.b requires the strain sensitivity of the observatory to comply with

$$\begin{aligned}
 \sqrt{S_h(f)} &< 2.2 \times 10^{-18} \text{ Hz}^{-1/2} & \text{at } f = 0.3 \text{ mHz} \\
 \sqrt{S_h(f)} &< 1.7 \times 10^{-20} \text{ Hz}^{-1/2} & \text{at } f = 3 \text{ mHz} \\
 \alpha &= 1.74 \times 10^{-19} & \beta = -2.10
 \end{aligned}
 \tag{MR 2.4b}$$

This requirement holds as long as the galactic confusion noise-like signal is at the level shown in figure 1.

**Rationale**

The threshold system for the ranges above is chosen with a mass ratio of  $q = 10^{-3}$ , a total intrinsic mass of  $10^6 M_\odot$  at  $z = 3$

Achieving a total **SNR** of 20 for the systems described in OR2.4.a requires the characteristic strain of the observatory to be below  $5 \times 10^{-20}$  at 0.3 mHz, falling to  $1.2 \times 10^{-21}$  at 3 mHz. It is taken as given that one can subtract galactic compact binary sources to the levels predicted here. This corresponds to saying that we require the instrument sensitivity to be below the galactic confusion noise over this frequency band.

Table 5: Graphical representation of OR2.4a. Parameters of the reference source are  $z = 0.8$ ,  $M_{\text{tot}} = 1000 M_{\odot}$ ,  $q = 1.0$ ,  $\chi = 0$ ; its maximum accumulated SNR is 23.2.

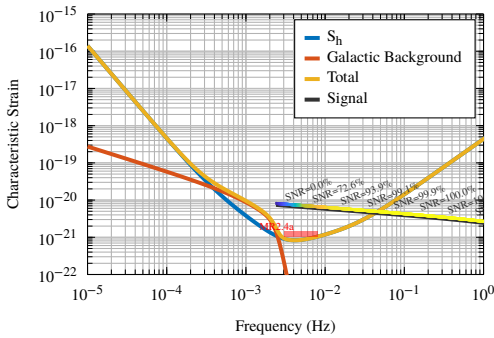


Figure 21: Frequency domain waveform of the reference source.

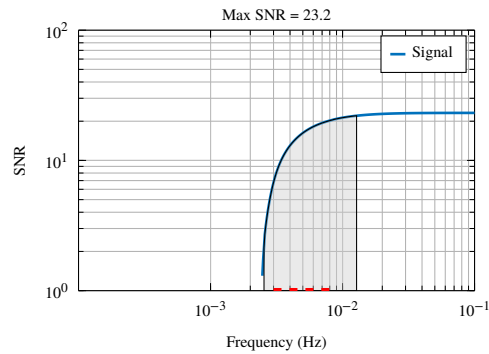


Figure 22: A plot of accumulated SNR versus frequency for the reference source.

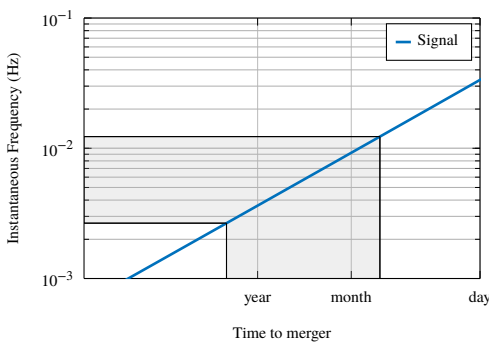


Figure 23: Instantaneous frequency of the reference source as a function of time to merger. The shaded region shows the time in-band.

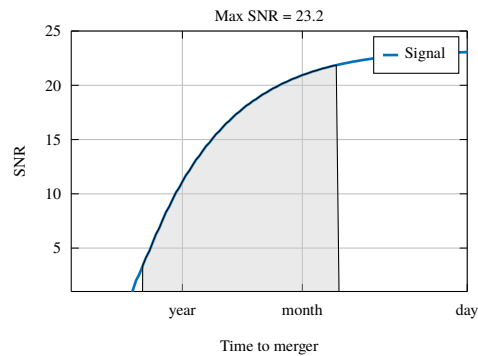


Figure 24: A plot of accumulated SNR versus time to merger for the reference source.

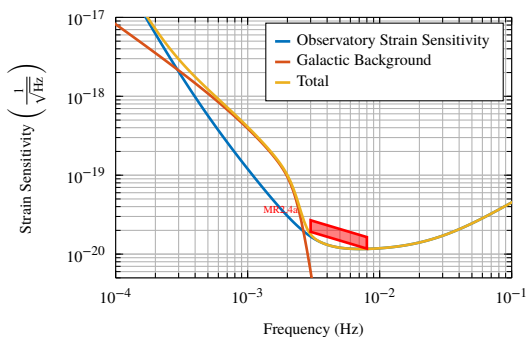


Figure 25: Strain sensitivity

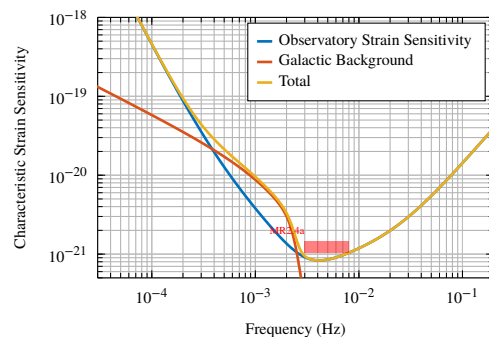


Figure 26: Characteristic strain sensitivity

Table 6: Graphical representation of OR2.4b. Parameters of the reference source are  $z = 4$ ,  $M_{\text{tot}} = 10^6 M_{\odot}$ ,  $q = 1 \times 10^{-3}$ ,  $\chi = 0$ ; its maximum accumulated SNR is 13.3.

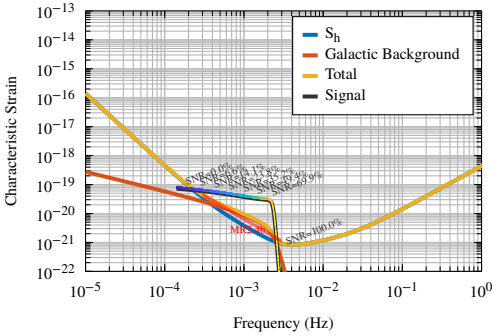


Figure 27: Frequency domain waveform of for the reference source.

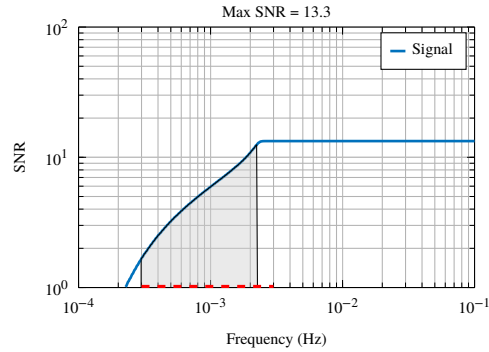


Figure 28: A plot of accumulated SNR versus frequency for the reference source.

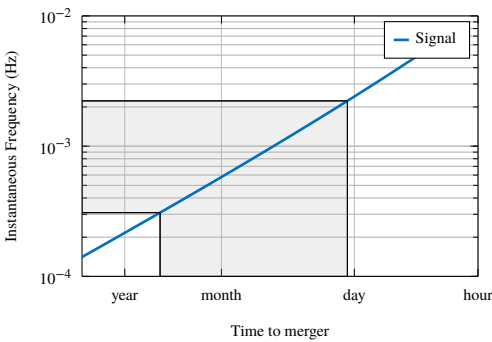


Figure 29: Instantaneous frequency of the reference source as a function of time to merger. The shaded region shows the time in-band.

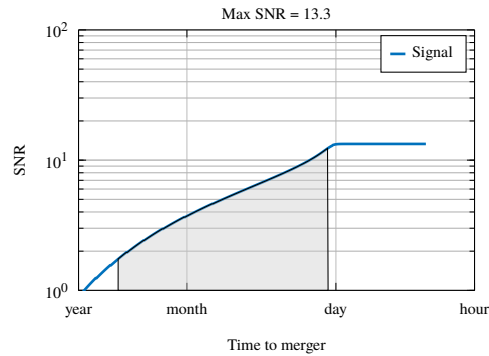


Figure 30: A plot of accumulated SNR versus time to merger for the reference source.

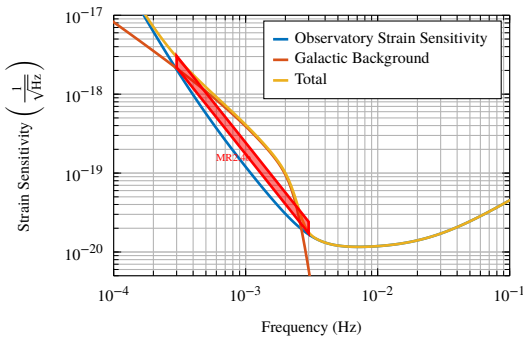


Figure 31: Strain sensitivity

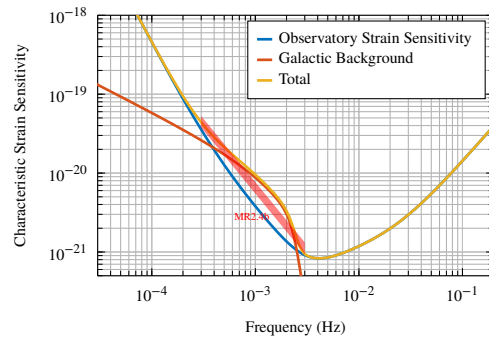


Figure 32: Characteristic strain sensitivity

### SO 3: Probe the dynamics of dense nuclear clusters using EMRIs

**EMRIs** describe the long-lasting inspiral (from months to a few years) and plunge of **SOBHs**, with mass range  $10 M_{\odot} - 60 M_{\odot}$ , into **MBHs** of  $10^5 M_{\odot} - 10^6 M_{\odot}$  in the centre of galaxies (Amaro-Seoane et al., 2007). The orbits of **EMRIs** are generic and highly relativistic. The **SOBH** spends  $10^3$  to  $10^5$  orbits in close vicinity of the **MBH** horizon, and the orbit displays extreme forms of periastron and orbital plane precession. The large number of orbital cycles allows ultra precise measurements of the parameters of the binary system as the **GW** signal encodes information about the spacetime of the central massive object. Considering the large uncertainty in the astrophysics of **EMRIs**, fulfillment of the requirements of this section would yield a minimum rate of one observed system per year, according to current most conservative **EMRI** population models.

#### *SI 3.1: Study the immediate environment of Milky Way like MBHs at low redshift*

##### **OR 3.1:**

Have the ability to detect **EMRIs** around **MBHs** with masses of a few times  $10^5 M_{\odot}$  out to redshift  $z = 3$  (for maximally spinning **MBHs**, and **EMRIs** on prograde orbits) with the **SNR** larger than 20. This enables an estimate of the redshifted, observer frame masses with the accuracy  $\delta M/M < 10^{-4}$  for the **MBH** and  $\delta m/m < 10^{-3}$  for the **SOBH**. Estimate the spin of the **MBH** with an accuracy of 1 part in  $10^3$ , the eccentricity and inclination of the orbit to one part in  $10^3$ .

##### **MR 3.1:**

A threshold system for the range in OR 3.1 would have a central non-spinning **MBH** with a mass of  $5 \times 10^5 M_{\odot}$ , a **SOBH** of  $10 M_{\odot}$  on a circular orbit, at redshift of  $z = 1.2$ . Such a system would have an accumulated **SNR** = 20 over a four year mission if the strain sensitivity of the observatory complies with

$$\begin{aligned}
 \sqrt{S_h(f)} &< 2.6 \times 10^{-20} \text{ Hz}^{-1/2} & \text{at } f &= 3 \text{ mHz} \\
 \sqrt{S_h(f)} &< 1.7 \times 10^{-20} \text{ Hz}^{-1/2} & \text{at } f &= 7 \text{ mHz} \\
 \alpha &= 4.46 \times 10^{-20} & \beta &= -0.500
 \end{aligned}
 \tag{MR 3.1}$$

All other systems with either lower redshift, higher component mass, or higher spin will produce a higher **SNR**. Systems with high spin and higher component mass may be detected out to redshift  $z = 4$ . Additionally we require the absence of any strong (**SNR** > 5) spectral lines of instrumental or environmental origin in the band from 2 mHz to 20 mHz, which could interfere with the harmonics of the **GW** signal from these systems. The plunge time will be known to high accuracy several months ahead. We require the capability of triggering a protected period of about one week around the plunge time to allow testing the accumulation of **SNR** against **GR**.

## SO 4: Understand the astrophysics of stellar origin black holes

Following the LIGO discovery of **SOBHs** in the mass range from  $10 M_{\odot}$  to  $30 M_{\odot}$  merging in binary systems in the nearby Universe, a new science objective arises for LISA, which was not originally part of *The Gravitational Universe*. Based on the inferred rates from the LIGO detections, fulfillment of the requirements of this section would allow LISA to individually resolve a minimum number of about 100 **SOBH** binaries, some of which would cross into the LIGO band weeks to months later, enabling multi-band GW astronomy (Sesana, 2016).

### *SI 4.1: Study the close environment of SOBHs by enabling multi-band and multi-messenger observations at the time of coalescence*

#### **OR 4.1:**

Have the ability to detect the inspiral signal from GW150914-like events with **SNR**  $> 7$  after 3 years of accumulated observation and estimate the sky localisation to better than  $1 \text{ deg}^2$  and the time of coalescence in ground-based detectors to within one minute for **TBD**% of the possible sky-locations and polarisations. This will allow the triggering of alerts to ground-based detectors and to pre-point **EM** probes at the **SOBH** coalescence.

#### **MR 4.1:**

Detecting the inspiral of **SOBHs** with a mass comparable to those in the GW150914 system with **SNR** higher than 7, accumulated over 4 years, constrains the rising branch of the sensitivity curve by requiring a strain sensitivity complying with

$$\begin{aligned}
 \sqrt{S_h(f)} &< 1.3 \times 10^{-20} \text{ Hz}^{-1/2} & \text{at } f &= 14 \text{ mHz} \\
 \sqrt{S_h(f)} &< 4.5 \times 10^{-20} \text{ Hz}^{-1/2} & \text{at } f &= 100 \text{ mHz} \\
 \alpha &= 2.24 \times 10^{-21} & \beta &= 0.652
 \end{aligned}
 \tag{MR 4.1}$$

#### **Rationale**

Detecting GW150914-like black holes with **SNR**  $\approx 7$  or higher accumulated over 4 years requires a strain sensitivity of better than  $1.4 \times 10^{-21}$  at 16 mHz rising to  $1 \times 10^{-21}$  at 100 mHz, assuming a duty cycle of 95 %.

### *SI 4.2: Disentangle SOBH binary formation channels*

#### **OR 4.2:**

Have the ability to observe **SOBH** binaries with total mass in excess of  $50 M_{\odot}$  out to redshift  $z = 0.1$ , with an **SNR** higher than 7 and a typical fractional error on the mass of 1 part in 100 and eccentricity with an absolute error of 1 part in  $10^{-3}$  for **TBD**% of the sky-positions, polarisations and inclinations.

Table 7: Graphical representation of OR4.1. Parameters of the reference source are  $z = 0.1$ ,  $M_{\text{tot}} = 63 M_{\odot}$ ,  $q = 0.8$ ,  $\chi = 0$ ; its maximum accumulated SNR is 3.7.

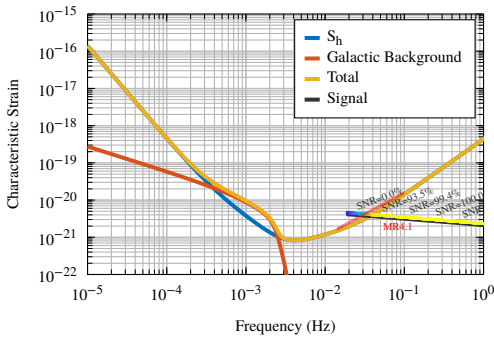


Figure 33: Frequency domain waveform of the reference source.

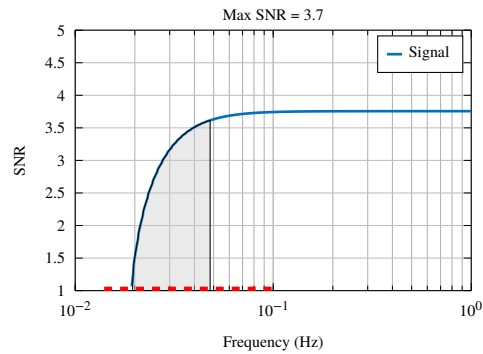


Figure 34: A plot of accumulated SNR versus frequency for the reference source.

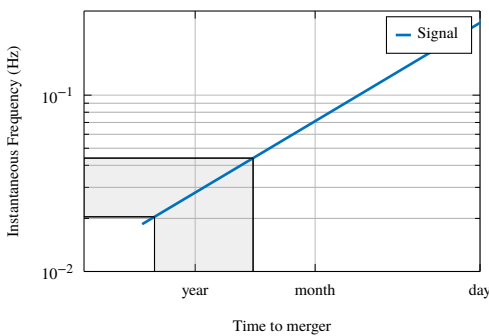


Figure 35: Instantaneous frequency of the reference source as a function of time to merger. The shaded region shows the time in-band.

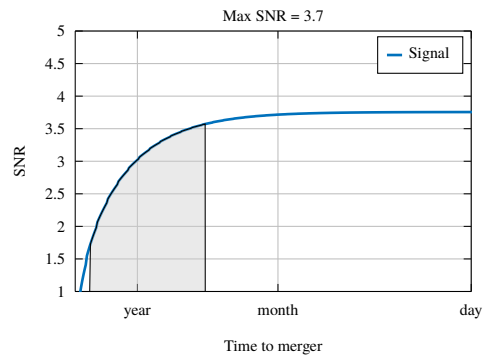


Figure 36: A plot of accumulated SNR versus time to merger for the reference source.

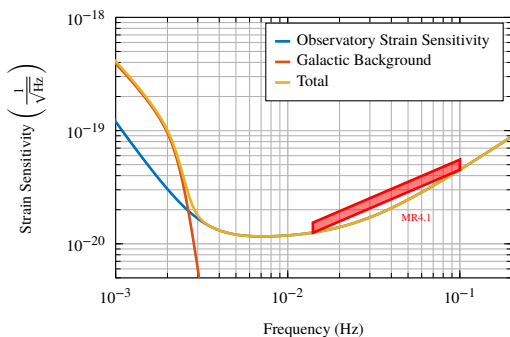


Figure 37: Strain sensitivity

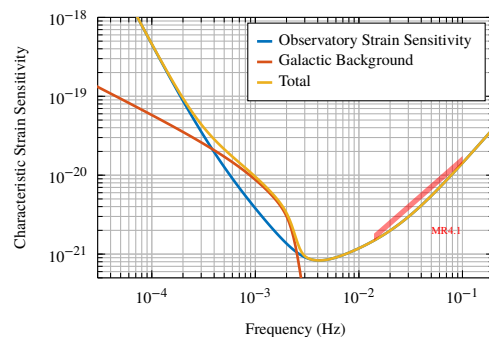


Figure 38: Characteristic strain sensitivity



**MR 4.2:**

OR 4.2 requires a strain sensitivity to comply with

$$\begin{aligned}\sqrt{S_h(f)} &< 1.5 \times 10^{-20} \text{ Hz}^{-1/2} && \text{at } f = 5 \text{ mHz} \\ \sqrt{S_h(f)} &< 1.5 \times 10^{-20} \text{ Hz}^{-1/2} && \text{at } f = 20 \text{ mHz} \\ \alpha &= 1.50 \times 10^{-20} && \beta = 0\end{aligned}\tag{MR 4.2}$$

## SO 5: Explore the fundamental nature of gravity and black holes

**MBHBs** and **EMRIs** enable us to perform tests of **GR** in the strong field regime and dynamical sector (Barack and Cutler, 2007; Berti et al., 2006). Precision tests such as these require “Golden” binaries, that is, **MBHBs** with very high (larger than 100) **SNR** in the post-merger phase or **EMRIs** with **SNR** > 50.

**SI 5.1: Use ring-down characteristics observed in MBHB coalescences to test whether the post-merger objects are the black holes predicted by GR.**

### OR 5.1

Have the ability to detect the post-merger part of the **GW** signal from MBHBs with  $M > 10^5 M_{\odot}$  out to high redshift, and observe more than one ring-down mode to test the “no-hair” conjecture of **GR**.

#### MR 5.1a:

The range of systems defined in OR 5.1 sets a constraint on the sensitivity curve by requiring the high **SNR** and the observation of the merger. For masses at the low end of the range, the threshold system is one out at  $z = 15$  with a mass of  $10^5 M_{\odot}$ , which will give an **SNR** of about 100 in the ringdown if the strain sensitivity complies to

$$\begin{aligned} \sqrt{S_h(f)} &< 1.6 \times 10^{-20} \text{ Hz}^{-1/2} & \text{at } f &= 3 \text{ mHz} \\ \sqrt{S_h(f)} &< 1.2 \times 10^{-20} \text{ Hz}^{-1/2} & \text{at } f &= 9 \text{ mHz} \\ \alpha &= 2.33 \times 10^{-20} & \beta &= -0.317 \end{aligned} \quad (\text{MR 5.1a})$$

### Rationale

The range of systems defined in OR5.1 sets a constraint on the sensitivity curve by requiring the high **SNR** and the observation of the merger. For masses at the low end of the range, the threshold system is one out at  $z = 15$  with a total mass of  $10^5 M_{\odot}$  with  $q = 0.2$  (see Figure 39). Such a system gives a total **SNR** of 100 in the baseline observatory configuration, about 70 % of which is in the ringdown (see figure 40). The **SNR** accumulated in the ringdown occurs in the band from about 3 mHz to 9 mHz. The system enters the band about 7 days prior to merger and merges at around 10 mHz (see figure 41).

#### MR 5.1b:

The contours of **SNR** in the mass/redshift plane are complicated, but we can constrain a point on the high mass end by considering a system of  $10^7 M_{\odot}$  out at redshift  $z = 4$ . This system constrains the strain sensitivity to

$$\begin{aligned} \sqrt{S_h(f)} &< 4.7 \times 10^{-17} \text{ Hz}^{-1/2} & \text{at } f &= 0.1 \text{ mHz} \\ \sqrt{S_h(f)} &< 1.9 \times 10^{-18} \text{ Hz}^{-1/2} & \text{at } f &= 0.31 \text{ mHz} \\ \alpha &= 6.67 \times 10^{-20} & \beta &= -2.85 \end{aligned} \quad (\text{MR 5.1b})$$

with the goal to extend this sensitivity down to low frequencies ( $f < 0.1$  mHz) to observe more of the inspiral phase, and to allow earlier detection. Systems with masses between these two end points are

Table 8: Graphical representation of OR5.1a. Parameters of the reference source are  $z = 15$ ,  $M_{\text{tot}} = 10^5 M_{\odot}$ ,  $q = 0.2$ ,  $\chi = 0$ ; its maximum accumulated SNR is 99.7.

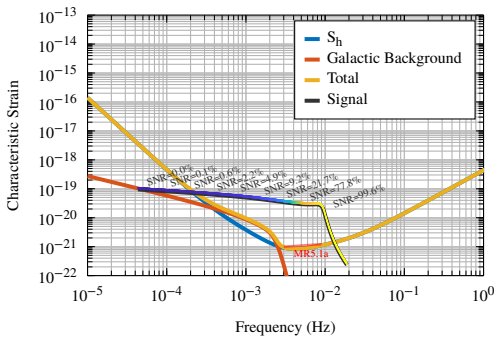


Figure 39: Frequency domain waveform of the reference source.

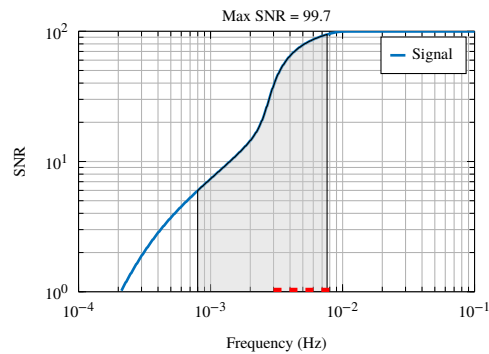


Figure 40: A plot of accumulated SNR versus frequency for the reference source.

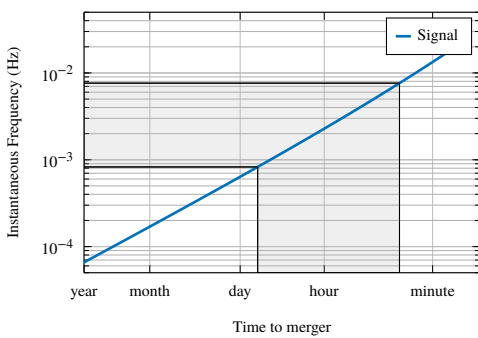


Figure 41: Instantaneous frequency of the reference source as a function of time to merger. The shaded region shows the time in-band.

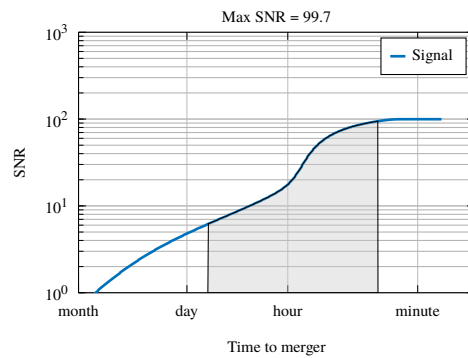


Figure 42: A plot of accumulated SNR versus time to merger for the reference source.

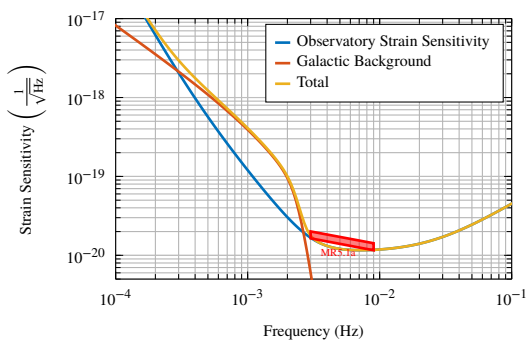


Figure 43: Strain sensitivity

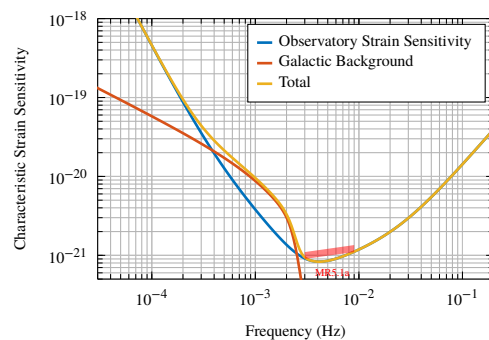


Figure 44: Characteristic strain sensitivity

considered “Golden” binaries, yielding **SNRs** of up to 1000 for systems out to redshift  $z = 3$ .

### **Rationale**

Due to the complexity of the **SNR** versus mass and redshift parameter space, we need to place a constraint using a system at the high mass end. So we set another threshold system of  $10^7 M_{\odot}$  at redshift  $z = 4$ , again with  $q = 0.2$ . Such a system enters the measurement band at around 50  $\mu\text{Hz}$ , and 0.4 mHz.

This system constrains the sensitivity of the observatory to be below  $3.5 \times 10^{-18}$  at 50 Hz, and below  $5 \times 10^{-20}$  at 0.3 mHz. This system will be detected with an **SNR** of 10 about 4 days prior to merger.

### ***SI 5.2: Use EMRIs to explore the multipolar structure of MBHs***

#### ***OR 5.2:***

Have the ability to detect “Golden” **EMRI** (those are systems from OR 3.1 with **SNR**  $> 50$ , spin  $a > 0.9$ , and in a prograde orbit) and estimate the mass of the **SOBH** with an accuracy higher than 1 part in  $10^4$ , the mass of the central **MBH** with an accuracy of 1 part in  $10^5$ , the spin with an absolute error of  $10^{-4}$ , and the deviation from the Kerr quadrupole moment with an absolute error of better than  $10^{-3}$ .

#### ***MR 5.2:***

The **MRs** are the same as MR3.1, but due to uncertainties in the astrophysical populations, a mission lifetime of several years is essential here to increase the chance of observing a Golden **EMRIs**.

### ***SI 5.3: Testing for the presence of beyond-GR emission channels***

Test the presence of beyond-**GR** emission channels (dipole radiation) to unprecedented accuracy by detecting GW150914-like binaries, which appear in both the LISA and LIGO frequency bands (Barausse et al., 2016). The **ORs** and **MRs** are the same as those in SI 4.1.

### ***SI 5.4: Test the propagation properties of GWs***

Test propagation properties of **GW** signals from **EMRIs** and from coalescing **MBHBs**. Detect the coalescence of Golden **MBHBs** (those systems described in OR 2.2 with an **SNR**  $> 200$ ) and have the ability to detect a Golden **EMRI** (as defined in OR 5.2) which allows us to constrain the dispersion relation and set upper limits on the mass of the graviton and possible Lorentz invariance violations. The **ORs** and **MRs** are the same as those in MR 2.2 and MR 3.1.

### ***SI 5.5: Test the presence of massive fields around massive black holes with masses larger than $10^3 M_{\odot}$***

Constrain the masses of axion-like particles or other massive fields arising in Dark-Matter models by accurately measuring the masses and spins of **MBHs** (Arvanitaki and Dubovsky, 2011). The requirements on the accuracy of the mass and spin measurements are the same as in SI 2.2.

Investigate possible deviations in the dynamics (encoded in the **GW** signal) of a solar mass object spiralling into an intermediate mass **IMBH** (mass smaller than a few  $10^4 M_{\odot}$ ) due to the presence of a Dark Matter mini-spike around the **IMBH** (Eda et al., 2015). This is a discovery project and the

Table 9: Graphical representation of OR5.1b. Parameters of the reference source are  $z = 4$ ,  $M_{\text{tot}} = 10^7 M_{\odot}$ ,  $q = 0.2$ ,  $\chi = 0$ ; its maximum accumulated SNR is 114.9.

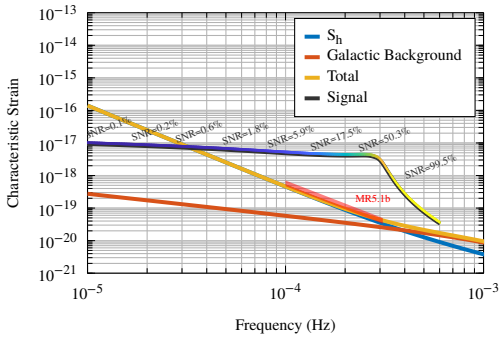


Figure 45: Frequency domain waveform of the reference source.

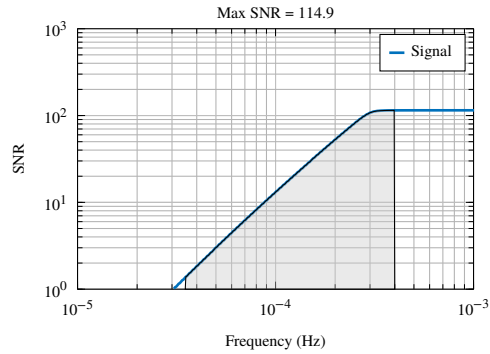


Figure 46: A plot of accumulated SNR versus frequency for the reference source.

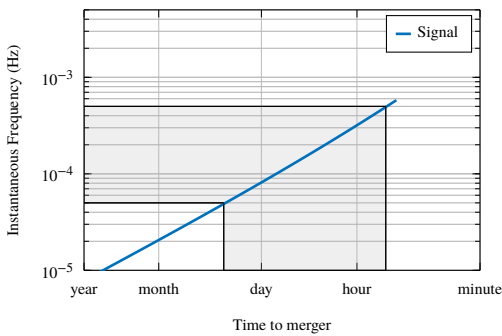


Figure 47: Instantaneous frequency of the reference source as a function of time to merger. The shaded region shows the time in-band.

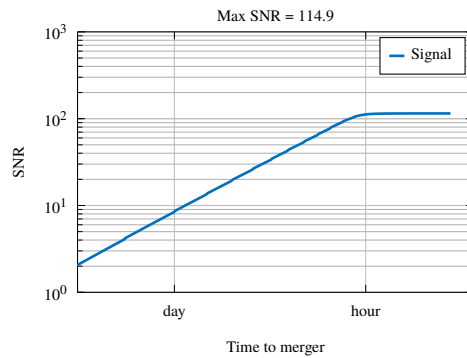


Figure 48: A plot of accumulated SNR versus time to merger for the reference source.

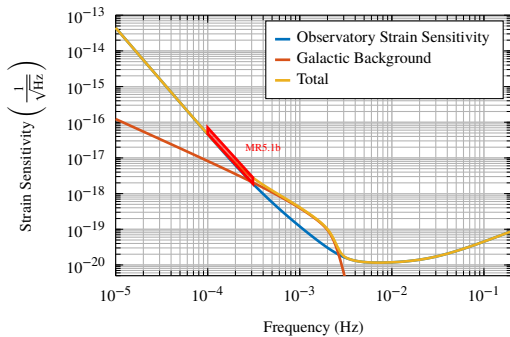


Figure 49: Strain sensitivity

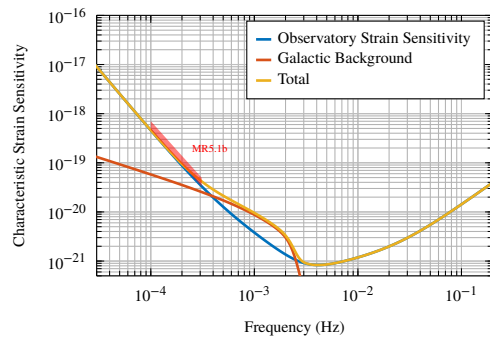


Figure 50: Characteristic strain sensitivity



high frequency requirements stated in MR 4.1, MR 4.2 make such a discovery possible for a **TBD**% of sources.

## SO 6: Probe the rate of expansion of the Universe

LISA will probe the expansion of the Universe using **GW** sirens at high redshifts: **SOBH** binaries ( $z < 0.2$ ), **EMRIs** ( $z < 1.5$ ), **MBHBs** ( $z < 6$ ).

### *SI 6.1: Measure the dimensionless Hubble parameter by means of **GW** observations only*

#### **OR 6.1a**

Have the ability to observe **SOBH** binaries with total mass  $M > 50 M_{\odot}$  at  $z < 0.1$  with **SNR** higher than 7 and typical sky location of better than  $1 \text{ deg}^2$ .

#### **OR 6.1b**

Have the ability to localize **EMRIs** with an **MBH** mass of  $5 \times 10^5 M_{\odot}$  and an **SOBH** of  $10 M_{\odot}$  at  $z = 1.5$  to better than  $1 \text{ deg}^2$ .

#### **MR 6.1:**

In terms of sensitivity curve, the OR 6.1a-b are automatically met if MR3.1 and MR4.1 are fulfilled. The need to collect a large enough sample of sources translates into a minimal mission duration requirement. According to current best population estimates, a 4 year mission is needed to yield a measurement of the Hubble parameter to better than 0.02, which helps resolving the tension among the values of the Hubble parameter determined with local Universe standard candles and with the Cosmic Microwave Background.

### *SI 6.2: Constrain cosmological parameters through joint **GW** and **EM** observations*

#### **OR 6.2**

Have the capability to observe mergers of **MBHBs** in the mass range from  $10^5 M_{\odot}$  to  $10^6 M_{\odot}$  at  $z < 5$ , with accurate parameter estimation and sky error of better than  $10 \text{ deg}^2$  to trigger **EM** follow ups (Tamanini et al., 2016).

#### **MR 6.2**

In terms of the sensitivity curve, OR 6.2 is automatically met if the **MRs** related to SO2 are fulfilled. The need to collect a large enough sample of sources translates into a minimal mission duration requirement. According to current best population estimates, a 4 year mission is needed to yield a measurement of the Hubble parameter to 0.01 and the dark energy equation of state parameter,  $w_0$ , to 0.1.

## SO 7: Understand stochastic GW backgrounds and their implications for the early Universe and TeV-scale particle physics

One of the LISA goals is the direct detection of a stochastic **GW** background of cosmological origin (such as the one produced by a first-order phase transition around the TeV scale) and stochastic foregrounds. Probing a stochastic **GW** background of cosmological origin provides information on new physics in the early Universe. The shape of the signal gives an indication of its origin, while an upper limit allows to constrain models of the early Universe and particle physics beyond the standard model.

For these investigations we need to ensure the availability of the data streams needed to form the Sagnac (or null-stream) TDI channel where the GW signal is partially suppressed in order to help separate the GW background from instrument noise.

### *SI 7.1: Characterise the astrophysical stochastic GW background*

#### **OR 7.1:**

Characterise the stochastic **GW** background from **SOBH** binaries and neutron star binaries with energy density normalised to the critical energy density in the Universe today,  $\Omega$ , based on the inferred rates from the LIGO detections, i.e., at the lowest  $\Omega = 4 \times 10^{-10} (f/25 \text{ Hz})^{2/3}$  (Abbott, 2017). This requires the ability to verify the spectral shape of this stochastic background, and to measure its amplitude in the frequency ranges  $0.8 \text{ mHz} < f < 4 \text{ mHz}$  and  $4 \text{ mHz} < f < 20 \text{ mHz}$ .

#### **MR 7.1:**

The **SNR** over the assumed 3 years of accumulated science observation must be larger than 10 **TBD** in the two frequency ranges. This corresponds to a strain sensitivity that complies with

$$\begin{aligned} \sqrt{S_h(f)} &< 3.5 \times 10^{-19} \text{ Hz}^{-1/2} & \text{at } f = 0.8 \text{ mHz} \\ \sqrt{S_h(f)} &< 1.4 \times 10^{-20} \text{ Hz}^{-1/2} & \text{at } f = 4 \text{ mHz} \\ \alpha &= 2.25 \times 10^{-19} & \beta = -2 \end{aligned} \quad (\text{MR 7.1a})$$

as well as with

$$\begin{aligned} \sqrt{S_h(f)} &< 1.5 \times 10^{-20} \text{ Hz}^{-1/2} & \text{at } f = 4 \text{ mHz} \\ \sqrt{S_h(f)} &< 1.5 \times 10^{-20} \text{ Hz}^{-1/2} & \text{at } f = 20 \text{ mHz} \\ \alpha &= 1.50 \times 10^{-20} & \beta = 0 \end{aligned} \quad (\text{MR 7.1b})$$

### *SI 7.2: Measure, or set upper limits on, the spectral shape of the cosmological stochastic GW background*

#### **OR 7.2:**

Probe a broken power-law stochastic background from the early Universe as predicted, for example, by first order phase transitions (Caprini, 2016) (other spectral shapes are expected, for example, for cosmic strings (*Report from the eLISA Cosmology Working Group*) and inflation (Bartolo, 2016)).



Therefore, we need the ability to measure  $\Omega = 2.8 \times 10^{-11} (f/10^{-4} \text{ Hz})^{-1}$  in the frequency ranges  $0.1 \text{ mHz} < f < 2 \text{ mHz}$  and  $2 \text{ mHz} < f < 15 \text{ mHz}$ , and  $\Omega = 8.0 \times 10^{-12} (f/10^{-2} \text{ Hz})^3$  in the frequency ranges  $2 \text{ mHz} < f < 15 \text{ mHz}$  and  $15 \text{ mHz} < f < 0.1 \text{ Hz}$ .

**MR 7.2:**

Ensure an **SNR** higher than 10 (**TBD**) over the 3 years of accumulated observation time in the three frequency ranges specified in OR 7.2 .

This would correspond to a strain sensitivity that complies to

$$\begin{aligned} \sqrt{S_h(f)} &< 7.1 \times 10^{-17} \text{ Hz}^{-1/2} && \text{at } f = 0.1 \text{ mHz} \\ \sqrt{S_h(f)} &< 4.0 \times 10^{-20} \text{ Hz}^{-1/2} && \text{at } f = 2 \text{ mHz} \\ \alpha &= 2.26 \times 10^{-19} && \beta = -2.50 \end{aligned} \quad (\text{MR 7.2a})$$

$$\begin{aligned} \sqrt{S_h(f)} &< 3.5 \times 10^{-20} \text{ Hz}^{-1/2} && \text{at } f = 2 \text{ mHz} \\ \sqrt{S_h(f)} &< 1.3 \times 10^{-20} \text{ Hz}^{-1/2} && \text{at } f = 15 \text{ mHz} \\ \alpha &= 4.96 \times 10^{-20} && \beta = -0.500 \end{aligned} \quad (\text{MR 7.2b})$$

$$\begin{aligned} \sqrt{S_h(f)} &< 1.4 \times 10^{-20} \text{ Hz}^{-1/2} && \text{at } f = 15 \text{ mHz} \\ \sqrt{S_h(f)} &< 9.4 \times 10^{-20} \text{ Hz}^{-1/2} && \text{at } f = 100 \text{ mHz} \\ \alpha &= 9.39 \times 10^{-22} && \beta = 1 \end{aligned} \quad (\text{MR 7.2d})$$

***Additional remarks***

Probing the gaussianity, the polarisation state, and/or the level of anisotropy of a potential stochastic background will give important information about the origin of the background. In particular, limiting the number of instrumental glitches will help to assess the gaussianity. The polarisation state shall be assessed with the three arm configuration. The measurement of the level of anisotropy depends on the frequency range and the amplitude of the background.

## **SO 8: Search for GW bursts and unforeseen sources**

LISA will lead us into uncharted territory, with the potential for many new discoveries. Distinguishing unforeseen, unmodelled signals from possible instrumental artifacts will be one of the main challenges of the mission, and will be crucial in exploring new astrophysical systems or unexpected cosmological sources.

### ***SI 8.1: Search for cusps and kinks of cosmic strings***

Searching for **GW** bursts from cusps and kinks of cosmic strings requires a deep understanding of the instrument noise and non-stationary behavior. Using the known shape of the bursts in the time and frequency domains will help to distinguish them from the instrumental artifacts and fluctuations in the stationarity of the instrument noise floor. Having the ability to use the Sagnac (or null-stream) TDI channels (**MR 7.2**) to veto such instrumental events will play a crucial role in the exploration of this discovery space.

### ***SI 8.2: Search for unmodelled sources***

Searching for **GW** bursts from completely unmodelled and unforeseen sources will also require a deep understanding of the instrument noise and non-stationary behavior. To distinguish such signals from instrumental effects, it is essential that sources of instrumental non-stationary artifacts be kept as few as possible and that we maintain the ability to form the Sagnac combination (which is insensitive to **GWs** at low frequencies). This requires that we maintain 6 laser links for the full duration of the mission (**MR 7.2**) and that we make available the necessary data streams to allow required computations on ground. This will help to veto out all non-**GW** burst-like disturbances.

Given the nature of this Science Investigation, no **MR** is levied on the instrument.

Table 10: Spectral indices and gains for the different MRs

MR	Frequency range		Gain	Spectral index
	$f_1$ (mHz)	$f_2$ (mHz)	$\alpha$ (Hz <sup>-1/2</sup> )	$\beta$
MR 1.1b	3	30	$8.37 \times 10^{-21}$	0.667
MR 1.1c	0.500	3	$1.73 \times 10^{-19}$	-1.83
MR 2.1	3	10	$2.19 \times 10^{-19}$	-0.261
MR 2.2	1	8	$1.23 \times 10^{-19}$	-0.993
MR 2.3	0.100	0.370	$7.86 \times 10^{-20}$	-2.76
MR 2.4a	3	8	$3.21 \times 10^{-20}$	-0.500
MR 2.4b	0.300	3	$1.74 \times 10^{-19}$	-2.10
MR 3.1	3	7	$4.46 \times 10^{-20}$	-0.500
MR 4.1	14	100	$2.24 \times 10^{-21}$	0.652
MR 4.2	5	20	$1.50 \times 10^{-20}$	0
MR 5.1a	3	9	$2.33 \times 10^{-20}$	-0.317
MR 5.1b	0.100	0.300	$6.67 \times 10^{-20}$	-2.85
MR 7.1a	0.800	4	$2.25 \times 10^{-19}$	-2
MR 7.2a	0.100	2	$2.26 \times 10^{-19}$	-2.50
MR 7.2b	2	15	$4.96 \times 10^{-20}$	-0.500
MR 7.2c	15	100	$9.39 \times 10^{-22}$	1

## B SUMMARY

Table 10 gives the gains  $\alpha$ , spectral indices  $\beta$  and the frequency range  $f_1 \leq f \leq f_2$  for the various MRs, following the common model

$$\sqrt{S_h(f)} < \alpha \left( \frac{f}{1 \text{ mHz}} \right)^\beta \quad \text{for } f_1 < f < f_2 \quad (5)$$

The piece-wise defined strains are for information only and do not constitute a sensitivity requirement.

## Acronyms

**AGN** active galactic nuclei.

**BH** black hole.

**EM** electro-magnetic.

**EMRI** extreme mass-ratio inspiral.

**GB** galactic binaries.

**GR** General Theory of Relativity.

**GW** gravitational wave.

**IMBH** intermediate-mass black hole.

**IMBHB** Intermediate Mass Black Hole Binary.

**LSST** Large Synoptic Survey Telescope.

**MBH** massive black hole.

**MBHB** massive black hole binary.

**MPR** mission performance requirement.

**MR** measurement requirement.

**OR** operational requirement.

**PSD** power spectral density.

**SI** science investigation.

**SNR** Signal-to-Noise Ratio.

**SO** science objective.

**SOBH** Stellar Origin Black Hole.

style = index

## References

- Abbott, BP et al. (2017). “GW170817: Implications for the Stochastic Gravitational-Wave Background from Compact Binary Coalescences”. In: arXiv: [1710.05837](https://arxiv.org/abs/1710.05837) [gr-qc].
- Amaro-Seoane, P et al. (2007). “TOPICAL REVIEW: Intermediate and extreme mass-ratio inspirals: astrophysics, science applications and detection using LISA”. In: *Classical and Quantum Gravity* 24, R113–R169. DOI: [10.1088/0264-9381/24/17/R01](https://doi.org/10.1088/0264-9381/24/17/R01). eprint: [astro-ph/0703495](https://arxiv.org/abs/astro-ph/0703495).
- Arvanitaki, A and S Dubovsky (2011). “Exploring the string axiverse with precision black hole physics”. In: *Phys. Rev. D* 83 (4), p. 044026. DOI: [10.1103/PhysRevD.83.044026](https://doi.org/10.1103/PhysRevD.83.044026).
- Barack, L and C Cutler (2007). “Using LISA extreme-mass-ratio inspiral sources to test off-Kerr deviations in the geometry of massive black holes”. In: *Phys. Rev. D* 75.4, 042003, p. 042003. DOI: [10.1103/PhysRevD.75.042003](https://doi.org/10.1103/PhysRevD.75.042003). eprint: [gr-qc/0612029](https://arxiv.org/abs/gr-qc/0612029).
- Barausse, E et al. (2016). “Theory-Agnostic Constraints on Black-Hole Dipole Radiation with Multiband Gravitational-Wave Astrophysics”. In: *Physical Review Letters* 116.24, 241104, p. 241104. DOI: [10.1103/PhysRevLett.116.241104](https://doi.org/10.1103/PhysRevLett.116.241104). arXiv: [1603.04075](https://arxiv.org/abs/1603.04075) [gr-qc].
- Barausse, E et al. *Report from the eLISA Cosmology Working Group*. Tech. rep. arXiv: [1601.07112](https://arxiv.org/abs/1601.07112) [astro-ph.CO].
- Bartolo, N et al. (2016). “Science with the space-based interferometer LISA. IV: Probing inflation with gravitational waves”. In: arXiv: [1610.06481](https://arxiv.org/abs/1610.06481) [astro-ph.CO].
- Berti, E et al. (2006). “Gravitational-wave spectroscopy of massive black holes with the space interferometer LISA”. In: *Phys. Rev. D* 73.6, 064030, p. 064030. DOI: [10.1103/PhysRevD.73.064030](https://doi.org/10.1103/PhysRevD.73.064030). eprint: [gr-qc/0512160](https://arxiv.org/abs/gr-qc/0512160).
- Caprini, C et al. (2016). “Science with the space-based interferometer eLISA. II: Gravitational waves from cosmological phase transitions”. In: *JCAP* 1604.04, p. 001. DOI: [10.1088/1475-7516/2016/04/001](https://doi.org/10.1088/1475-7516/2016/04/001). arXiv: [1512.06239](https://arxiv.org/abs/1512.06239) [astro-ph.CO].
- Danzmann, K and the LISA Consortium (2013). “The Gravitational Universe”. In: <https://arxiv.org/abs/1305.5720>.
- Eda, K et al. (2015). “Gravitational waves as a probe of dark matter minispikes”. In: *Phys. Rev. D* 91.4, 044045, p. 044045. DOI: [10.1103/PhysRevD.91.044045](https://doi.org/10.1103/PhysRevD.91.044045). eprint: [gr-qc/0612029](https://arxiv.org/abs/gr-qc/0612029).
- Klein, A et al. (2016). “Science with the space-based interferometer eLISA: Supermassive black hole binaries”. In: *Phys. Rev. D* 93.2, 024003, p. 024003. DOI: [10.1103/PhysRevD.93.024003](https://doi.org/10.1103/PhysRevD.93.024003). arXiv: [1511.05581](https://arxiv.org/abs/1511.05581) [gr-qc].
- Nelemans, G et al. (2001). “The gravitational wave signal from the Galactic disk population of binaries containing two compact objects”. In: *Astronomy & Astrophysics* 375, pp. 890–898. DOI: [10.1051/0004-6361:20010683](https://doi.org/10.1051/0004-6361:20010683). eprint: [astro-ph/0105221](https://arxiv.org/abs/astro-ph/0105221).
- Planck Collaboration et al. (2016). “Planck 2015 results. XIII. Cosmological parameters”. In: *A&A* 594, A13, A13. DOI: [10.1051/0004-6361/201525830](https://doi.org/10.1051/0004-6361/201525830). arXiv: [1502.01589](https://arxiv.org/abs/1502.01589).
- Portegies Zwart, SF and SLW McMillan (2002). “The Runaway Growth of Intermediate-Mass Black Holes in Dense Star Clusters”. In: *The Astrophys. J.* 576, pp. 899–907. DOI: [10.1086/341798](https://doi.org/10.1086/341798). eprint: [astro-ph/0201055](https://arxiv.org/abs/astro-ph/0201055).
- Sesana, A (2016). “Prospects for Multiband Gravitational-Wave Astronomy after GW150914”. In: *Physical Review Letters* 116.23, 231102, p. 231102. DOI: [10.1103/PhysRevLett.116.231102](https://doi.org/10.1103/PhysRevLett.116.231102). arXiv: [1602.06951](https://arxiv.org/abs/1602.06951) [gr-qc].
- Sesana, A et al. (2004). “Low-Frequency Gravitational Radiation from Coalescing Massive Black Hole Binaries in Hierarchical Cosmologies”. In: *The Astrophysical Journal* 611.2, p. 623.



- Tamanini, N et al. (2016). “Science with the space-based interferometer eLISA. III: Probing the expansion of the Universe using gravitational wave standard sirens”. In: *JCAP* 1604.04, p. 002. DOI: [10.1088/1475-7516/2016/04/002](https://doi.org/10.1088/1475-7516/2016/04/002). arXiv: [1601.07112](https://arxiv.org/abs/1601.07112) [astro-ph.CO].
- Toonen, S et al. (2012). “Supernova Type Ia progenitors from merging double white dwarfs: Using a new population synthesis model”. In: *Astron. Astrophys.* 546, A70. DOI: [10.1051/0004-6361/201218966](https://doi.org/10.1051/0004-6361/201218966). arXiv: [1208.6446](https://arxiv.org/abs/1208.6446) [astro-ph.HE].
- Volonteri, M (2010). “Formation of supermassive black holes”. In: *The Astronomy and Astrophysics Review* 18, pp. 279–315. DOI: [10.1007/s00159-010-0029-x](https://doi.org/10.1007/s00159-010-0029-x). arXiv: [1003.4404](https://arxiv.org/abs/1003.4404).